

**Assessment of Seismic Response of Masonry Piers and Characterization of
their Seismic Damage under Dynamic Load Simulations**



by

**Muhammad Yousaf Anwar
(2011–NUST–MS PhD–STR–08)**

This thesis is submitted in partial fulfillment of
the requirements for the degree of

Master of Science

in

Structural Engineering

National Institute of Civil Engineering (NICE)

School of Civil & Environmental Engineering (SCEE)

National University of Sciences and Technology (NUST)

Islamabad, Pakistan

(2013)

**Assessment of Seismic Response of Masonry Piers and Characterization
of their Seismic Damage under Dynamic Load Simulations**

by

Muhammad Yousaf Anwar

A Thesis of

Master of Science in Structural Engineering

Submitted to the

National Institute of Civil Engineering (NICE)

School of Civil & Environmental Engineering (SCEE)

National University of Sciences and Technology (NUST)

Islamabad, Pakistan

In partial fulfillment of the requirements

for the degree of

Master of Science in Structural Engineering

(2013)

DEDICATED TO

MY PARENTS

ACKNOWLEDGEMENTS

All praise to Almighty Allah who gave the courage and power to the author for completing this research work.

I pay my earnest gratitude with sincere sense of respect to my parents and siblings for their unending support, encouragement, prayers and patience.

Foremost, I am heartily thankful to my supervisor Assoc. Prof. Dr. Abdul Qadir Bhatti, SCEE, whose guidance, support and patience from initial to final level made it possible for me to complete this work. Without his technical and moral support the completion of this work was impossible.

The author expresses his utmost gratitude to Prof. Dr. Muhammad Asghar Bhatti, University of Iowa, USA. The author got excellent training and knowledge about ANSYS and MATLAB from Dr. M.A. Bhatti during the latter's visit to RCMS for instruction of a course on non-linear Finite Element analysis of solids and structures. Prof. M.A. Bhatti facilitated the author in getting exposure to all relevant tools and techniques for completing this study of assessment of seismic response of structures.

The author is grateful to Dr. Shaukat Ali Khan and Dr. Wasim Khaliq for their valuable suggestions and guidance throughout the study period. They provided enough support during the modeling work and gave precious suggestions while reviewing the thesis.

The author would like to thank Dr. Yasar Ayaz for his technical support in the Finite Element Modeling work and data processing. He helped a lot in the fabrication of the Finite Element model and extended his support in the analysis of the model results

ABSTRACT

This research intends to the formulation of a finite element model for predicting the seismic response of masonry bridge piers. Cyclic load simulations are to be applied to the model and the stress-strain hysteretic graphs and contour plots of base shear, isolation system displacements, strain-energies and lateral drift are to be examined to have an insight into variation of dynamic response with increase in the forcing functions. This would also provide knowledge about the type of damage the structure underwent and characterization of this damage. Alternatively, the data obtained can also be beneficially employed for economically viable retrofitting/strengthening of such bridges (or other structures).

Keeping in view the abundance of masonry buildings/bridges (both brick and stone) in Pakistan, a thorough and in-depth understanding of masonry structures is needed. Earthquakes had brought huge significance to the evaluation of buildings/bridges for their performance in events of ground motions.

Experiments on models of masonry buildings/bridges have been performed in the past but the results are largely applicable only to the type of structures that resemble, in material and testing conditions, with the tested models. Numerical modeling of masonry is a demanding task but it provides researcher with the room to evaluate the behavior of such structures for a diverse set of loading conditions and for a variety of materials having different mechanical properties.

This very diversity justifies this research's FEM based dynamic analysis of masonry structures, including bridges. Such type of FEM model is also a tool that can cater for the demand of analysis of a high number of different buildings/bridges with geometry and material varying from each other. The model can hence be modified accordingly for such structures and results can be obtained with convenience regarding the characterization of damage to such structures.

TABLE OF CONTENTS

| | |
|--|-----------|
| CHAPTER 1 | 1 |
| 1.1 introduction | 1 |
| 1.2 Background and Need For Research..... | 3 |
| 1.3 Objectives of this Study | 5 |
| CHAPTER 2 | 8 |
| 2.1 General | 8 |
| 2.2 Seismic Performance Evaluation of Unreinforced Masonry Buildings..... | 10 |
| 2.3 In-Plane Failure Modes in Unreinforced Masonry Walls..... | 11 |
| 2.4 Toe Crushing/Rocking Failure Mode in URM Walls..... | 12 |
| 2.5 Sliding Shear Failure Mode in URM Walls..... | 13 |
| 2.6 Diagonal Tension Shear Failure Mode in URM Walls..... | 13 |
| 2.7 Confined masonry | 14 |
| 2.8 Plane Failure of Confined Masonry Buildings | 15 |
| 2.8 Connection failure..... | 16 |
| 2.9 Seismic Damage Assessment..... | 17 |
| 2.10 Seismic Vulnerability Assessment of Buildings..... | 17 |
| 2.11 Observed Vulnerability..... | 18 |
| 2.12 Expert Opinions Based Seismic Damage Assessment..... | 19 |
| 2.13 Simple Analytical Models Based Evaluation of Damage to Masonry Buildings..... | 19 |
| 2.14 Advanced Capacity Spectrum Method | 21 |
| CHAPTER 3 | 23 |
| 3.1 General..... | 23 |
| 3.2 Static monotonic and quasi-static loading | 23 |
| 3.3 Dynamic Tests using shakes Table | 24 |
| 3.4 Pseudo-dynamic method..... | 25 |
| 3.5 Findings from previous tests carried out on masonry structures | 26 |
| 3.6 Shaking table investigation of masonry houses, University of California, Berkeley USA | 27 |
| 3.7 Masonry walls subjected to shake table testing; University of Pavia, Italy..... | 28 |

| | |
|---|-----------|
| 3.8 Masonry and Adobe Houses Shake Table Tests; Stanford University California, USA..... | 29 |
| 3.9 Correlation between Dynamic and static behavior of masonry structure; UIUC, USA | 29 |
| 3.10 Experimental Investigations on masonry walls; Institute fur Massivbau, Germany | 30 |
| 3.11 Masonry Materials and Properties | 31 |
| 3.12 Buckling and Material Overstressing..... | 32 |
| 3.13 Analytical and Numerical Approaches | 33 |
| 3.14 Softening Behavior of Masonry | 34 |
| CHAPTER 4----- | 35 |
| 4.1 Introduction..... | 35 |
| 4.2 Adopted Modeling Strategy | 35 |
| 4.3 Finite Element Analysis of Stone Masonry | 37 |
| 4.4 Mesh Generation and Element Selection | 38 |
| 4.5 Material Properties (Strength, Elastic and Inelastic Parameters)..... | 40 |
| 4. 6 Geometry Definition | 43 |
| 4.7 Definition Of The Linear Properties Of The Material | 44 |
| 4.8 Numerical Analysis..... | 47 |
| 4.9 Linear Static Analysis | 48 |
| 4.10 FEM Analysis Results..... | 48 |
| 4.11 Modes of Failure | 49 |
| 4.12 Load-Displacement Curves..... | 54 |
| 4.13 Variation in Material Properties' Parameters | 60 |
| 4.14 Boundary Condition and Loading..... | 64 |
| 4.15 Validation of Model | 66 |
| CHAPTER 5 ----- | 76 |
| 5.1 General | 76 |
| 5.2 Conclusions..... | 77 |
| 5.4 Recommendations..... | 78 |
| REFERENCES ----- | 79 |

LIST OF FIGURES

| | |
|--|----|
| Figure 2.1. Load resisting mechanism of masonry structures | 9 |
| Figure 2.2. Reaction of masonry to seismic loads | 10 |
| Figure 2.3. Toe crushing failure..... | 12 |
| Figure 2.4. Sliding Shear Failure | 13 |
| Figure 2.5. Diagonal flexural failure..... | 14 |
| Figure 2.6. Typical confined masonry | 15 |
| Figure 2.7. Cracking in confined masonry under monotonic gravity loads..... | 16 |
| Figure 2.8. (a) Overturning failure (b) Connection failure | 20 |
| Figure 2.9. Spectral displacement in masonry structures | 22 |
| Figure 3.1. Model being tested on shake table..... | 24 |
| Figure 3.2. A typical shake table with hydraulic actuators..... | 25 |
| Figure 3.3. Setup for pseudo dynamic testing..... | 26 |
| Figure 3.4. Graphical representation of buckling of masonry piers and walls | 33 |
| Figure 4.1. Element plot of FE model..... | 39 |
| Figure 4.2. Lines plot of FE Model..... | 40 |
| Figure 4.3. Force vs Drift for Case I..... | 42 |
| Figure 4.4. Nodes for the FE model..... | 44 |
| Figure 4.5. Cyclic application of vertical load only..... | 46 |
| Figure 4.6. Multi Plot of the FE model..... | 47 |
| Figure 4.7. Contour plot for XY principal shear..... | 49 |
| Figure 4.8. Contour Plot for ZY principal shear..... | 50 |
| Figure 4.9. Contour Plot of model when subjected to uniaxial monotonic loads only..... | 50 |

| | |
|---|----|
| Figure 4.10. Contour plot for ZX principal shear | 51 |
| Figure 4.11. Contour plot for principle shear in Y direction | 52 |
| Figure 4.12. Cracking Pattern in actual specimen | 52 |
| Figure 4.13. Contour plot for elastic strain in X axis..... | 53 |
| Figure 4.14. Displacement of top surface of FE model when subjected to first cycle of loading | 54 |
| Figure 4.15. Force-Displacement Curve for Case I | 55 |
| Figure 4.16. (a) Elemental Plot of crack, showing initial cracks in toe of the pier | 55 |
| Figure 4.16. (b) Elastic strain during 1st cycle of loading..... | 56 |
| Figure 4.17. Elastic strain during 2nd cycle of loading | 57 |
| Figure 4.19. Propagation of cracks | 57 |
| Figure 4.18. Principle Stress Concentration at toe of Wall..... | 58 |
| Figure 4.20. Cracking pattern in Actual specimen | 58 |
| Figure 4.21. Stress intensity for 1st cycle of loading..... | 59 |
| Figure 4.22. Stresss-Strain Plot of the entire model for Case I..... | 59 |
| Figure 4.23. Displacement with respect to Time for entire loading of the model in Case I..... | 59 |
| Figure 4.24. Comparison of numerical and experimental results for Case I | 60 |
| Figure 4.25. Nodal plot for Case II..... | 60 |
| Figure 4.26. Elemental plot for Case II..... | 61 |
| Figure 4.27. Displacement for top surface of pier for Case II | 62 |
| Figure 4.28. Elastic Strain plot for 2nd cycle of loading for Case II..... | 63 |
| Figure 4.29. Force displacement curve for Case II..... | 63 |
| Figure 4.30. Comparison of numerical and experimental results for Case II..... | 64 |
| Figure 4.31. 1st prinipal stress for 1st cycle for Case II | 65 |
| Figure 4.32. Storey Drift vs Force diagram for Case II..... | 65 |

| | |
|--|----|
| Figure 4.33. XY shear stain plot for 3rd cycle of loading for Case II | 65 |
| Figure 4.34. 3rd Principal Stress plot for Case II | 66 |
| Figure 4.35. Z Shear Stress plot for Case II..... | 66 |
| Figure 4.36. XY Shear plot for Case II..... | 67 |
| Figure 4.37. Stress intensity for (a) 2nd cycle of loading (b) 3rd cycle of loading | 67 |
| Figure 4.38. Cracking pattern under 2nd cycle of loading | 67 |
| Figure 4.39. Comparison of Stress Concentration and Cracking pattern | 68 |
| Figure 4.40. Comparison of Stress Concentration and Cracking patterns at higher loads | 68 |
| Figure 4.41. Storey Drift vs Force diagram for Case III..... | 70 |
| Figure 4.42. Time history of 2nd principle stress for Case III..... | 70 |
| Figure 4.43. Time history of 3rd principle stress for Case III | 71 |
| Figure 4.44. Time history of XY shear stress for Case III..... | 72 |
| Figure 4.45. Time history of XY shear elastic stain for Case III..... | 72 |
| Figure 4.46. Time history of Y component of force for Case III..... | 73 |
| Figure 4.47. Convergence values for Force for Case III..... | 73 |
| Figure 4.48. Comparison of numerical and experimental results for Case III..... | 74 |
| Figure 4.49. Convergence values for Displacement for Case III..... | 74 |
| Figure 4.50. Principle Stresses build up at center and cracks in center of actual specimen | 75 |
| Figure 4.51. Comparison of cracks propagation at toe in model and actual specimen..... | 75 |

NOMENCLATURE

| | | |
|------|---|---|
| a | : | Acceleration |
| Abm | : | Total shear area of brick mortar joints in between two bricks |
| Ag | : | Age of Building, years |
| An | : | Prism net area |
| Av | : | Shear area of masonry pier |
| Aw | : | Area of horizontal cross section of wall |
| A | : | Net area |
| ai | : | Acceleration of the ith mass |
| b | : | Shear stress distribution factor |
| Bb | : | Width of the brick |
| c | : | Cohesion |
| Cd | : | Displacement amplification factor |
| d | : | Displacement |
| du | : | Ultimate displacement |
| de | : | Elastic displacement |
| Ed | : | Dissipated energy |
| Einp | : | Input energy |
| Em | : | Modulus of elasticity |
| fb | : | Compressive strength of brick |
| fbt | : | Modulus of rupture |
| fmo | : | Compressive strength of mortar |
| fn | : | Resonant frequency |
| ft | : | Tensile Strength |
| ftu | : | Masonry specimen principal tensile strength |
| Gm | : | Modulus of rigidity |
| g | : | Ground acceleration |
| h | : | Height of pier |
| H | : | Height of specimen in diagonal compression test |

| | | |
|---------|---|---|
| He | : | Elastic load |
| Hu | : | Ultimate design load |
| k | : | Effective stiffness of bilinear curve |
| Ke | : | Effective stiffness |
| KP | : | Stiffness of pier |
| t | : | Thickness of the wall |
| Lp | : | Length of masonry pier |
| m | : | Mass |
| M | : | Mass matrix |
| Mcent | : | Bending moment at the mid span of the brick |
| Mw | : | Magnitude of earthquake |
| P | : | Applied load |
| PD | : | Vertical load |
| Pu | : | Ultimate vertical load |
| Psi | : | Pound per square inch |
| Pcf | : | Pound per cubic feet |
| Qp | : | Physical quantity of prototype |
| Qm | : | Physical quantity of model |
| R | : | Response modification factor |
| Sa | : | Spectral acceleration of single degree of freedom system |
| Sd | : | Spectral displacement of single degree of freedom system |
| SF | : | Scale factor for model |
| Sb | : | Brick section modulus |
| Ss | : | Average shear stress along the vertical diagonal |
| t | : | Thickness of specimen in diagonal compression test |
| Tb | : | Thickness of the brick |
| v | : | Velocity |
| Vb | : | Base shear |
| Vs | : | Shear wave velocity |
| Vus | : | Force required for producing shear sliding in the triplet prism |
| β | : | Ratio of effective stiffness to elastic stiffness of pier |

ABBREVIATIONS

| | | |
|-------|---|---|
| AR | : | Aspect Ratio |
| ASCE | : | American Society of Civil Engineers |
| ASTM | : | American Society for Testing and Materials |
| ATC | : | Applied Technology Council |
| CLSSr | : | Cement-Lime-Sand-Surkhi |
| CP | : | Collapse Prevention |
| COD | : | Coefficient of Determination |
| DSHA | : | Deterministic Seismic Hazard Analysis |
| EC | : | Eurocode |
| EEC | : | Earthquake Engineering Center |
| EERI | : | Earthquake Engineering and Research Institute |
| EEFIT | : | Earthquake Engineering Field Investigation Team |
| GI | : | Galvanized Iron gm |
| IAEE | : | International Association of Earthquake Engineers |
| IO | : | Immediate occupancy IRA |
| Kg | : | Kilogram |
| KN | : | Kilo Newton |
| ksi | : | Kilo pound per square inch |
| Lbs | : | Pounds |
| LS | : | Life Safety |
| LVDT | : | Linear Variable Displacement Transformer |
| LSSr | : | Lime-Sand-Surkhi |
| LS | : | Lime Sand |
| MAEC | : | Mid America Earthquake Centre |
| MASW | : | Multi-Channel Analysis of Surface Waves |
| MDOF | : | Multi Degree of Freedom mm |
| MMI | : | Modified Mercalli Intensity Scale |
| Mpa | : | Mega Pascal |
| NEHRP | : | National Earthquake Hazards Reduction Program |

| | |
|-----------|--|
| NESPAK : | National Engineering Services of Pakistan |
| NGA : | Next Generation Attenuation |
| NISRAF: | NEES Integrated Seismic Risk Assessment Framework |
| NMC : | Natural Moisture Content |
| NTC-M: | Mexico City Building Code |
| PEER DB : | Pacific Earthquake Engineering Research Centre Data Base |
| PGA : | Peak Ground Acceleration |
| PGD : | Peak Ground Displacement |
| PGV : | Peak Ground Velocity |
| PI : | Plasticity Index |
| PMD : | Pakistan Metrological Department |
| PS : | Peak Spectral Acceleration |
| Psd : | Pseudo dynamic |
| PUCP : | Catholic University of Peru |
| R : | Reinforced Concrete |
| SDOF : | Single Degree of Freedom |
| SPT : | Standard Penetration Test |
| UBC : | Uniform Building Code |
| UET : | University of Engineering and Technology |
| URM : | Unreinforced Masonry |
| URBM: | Unreinforced Brick Masonry |
| URCBM: | Unreinforced Concrete Block Masonry |
| USGS : | United States Geographical Survey |
| UTM : | Universal Testing Machine |

CHAPTER 1

INTRODUCTION

1.1 INTRODUCTION

Pakistan is home to three large mountain ranges i.e. Himalayas Mountain Range, Karakoram Mountain Range and Hindukush Mountain Range. Out of these, the Himalayan Mountains are known for its frequent seismic activity. Databases reveal that many natural seismic events of moderate magnitudes (i.e., $M_w = 5.0$ to 5.5) have been recorded in this part of the world. The recent 2005 Kashmir Earthquake ($M_w = 7.6$) rendered about 450,000 buildings damaged (ADB-WB, 2005). Out of these most of the buildings were non-engineered, un-reinforced masonry, including adobe, rubble stone and brick masonry buildings.

The damaged infrastructure also included small to medium sized bridges, constructed with stone or brick masonry. Collapse of such bridges created a hurdle in the provision of emergency services to the affected masses/areas. Many elements contributed towards the large magnitude of damage to infrastructure, e.g. structural configurations, low quality of masonry materials, workmanship and lack of confinement of the masonry walls (Naseer, A., et al, 2009). This revealed the fact that the currently practiced construction methods do not take into account some basic engineering aspects and cannot be termed appropriate unless a thorough analysis of such building methods/materials is carried out. The seismic damage to structures can be mitigated through analysis of such structures and thereafter, subjecting such structures to retrofitting and repair. It is, therefore, necessary to undertake an analysis of deficient buildings through experimental and numerical computational methods.

The severe earthquake, ($M_w = 7.6$) hit the Northern Areas of Pakistan in 2005. The event was catastrophic in terms of the huge loss it incurred on human life and national economy. As per the findings of World Bank, the calamity caused an economic loss of more than 5 billion US dollars. The building stock of the affected areas was mainly made up of stone and brick masonry. After the initiation of relief and rehabilitation works, there were demands from many stake holders to

undertake studies on the performance, analysis and future design of masonry structures in the subject location.

The seismic event also caught eye of researchers so that studies could be initiated in order to assess the building stock of that particular locality and to propose measures that would, to a humanly possible extent, lessen the damages to civil infrastructure. Consequently, a series of experimental studies were started for this purpose. New academic courses were initiated at Military College of Engineering, Risalpur and experiments were conducted at University of Engineering and Technology, Peshawar. This dissertation is focused on the evaluation of seismic performance of masonry structures of Pakistan through finite element numerical modeling.

As far as the damage to masonry structures is concerned, columns or piers and walls are of prime significance and, therefore, needs attention of researchers in areas of mechanics of such structural elements. Load bearing structural elements made up stone or brick masonry may fail due to instability. Mainly the failure is due to crushing of the constituent material or the bond failure between building blocks i.e. stones or bricks. In case of seismic events, the prediction of crushing loads and the characterization of damage to such structural elements can be done effectively through numerical modeling. However, the degree of precision of such finite element models is largely based on the model used to analyze the failure and the element properties that are used to model the masonry units. For sake of better insight into the characteristic of structural masonry, it is of significance to have an in-depth knowledge of constitutive laws of the building blocks such as stones, bricks, mortars etc. Due to issues of convenience, it is however, suggested that a reasonable simplification may be put in place by assuming that the subject masonry will behave as a continuum medium. Once this assumption is properly incorporated into the finite element model, an average stress-strain formulation can be considered for stones/bricks and the binding mortar.

Of all the factors affecting masonry construction, availability of materials and ease of operations are of prime importance. In normal construction, beams act primarily as flexural members whereas columns/piers and load bearing walls act as compression members. Under normal circumstances, masonry piers and walls carries vertical gravity loads from the above-lying structures. They are also subjected to incidental moments that are caused by continuity between walls and floor-slabs and also due to eccentricities in vertically applied loads. In cases where

masonry walls and piers are load bearing structures, they are aligned vertically for the height of a given structure. This ensures the transmittal of vertical loads to the foundation. The vertical loads, hence, cause a pre-stressing force in the piers and walls and enhance its capacity to cracking. Slender walls are prone to combined loading effect of vertical plus lateral loads because of the load eccentricity which may cause failure in the lateral direction. This is one of the major reasons that demands that analysis of structural masonry should be carried out by taking into account the characteristic behavior of building units i.e. stones and bricks and the binding mortar materials when subjected to a combination of axial loads, lateral loads and tension caused by eccentricity of loads.

Alternatively, it also calls for design of structural masonry by incorporating the effects of various forms of loads.

1.2 BACKGROUND AND NEED FOR RESEARCH

Much research has been done in the areas of design and analysis of masonry structural components with emphasis primarily being on masonry walls. Previously there has been an absence of a mechanism or model that could analyze the load-deformation of masonry piers and walls in their entirety. Different combinations of geometry, material features and loading scenarios lead to different mechanisms of failures and each needed to be studied in depth to propose a viable model for each one of them. One of the approaches is to take into account both sorts of nonlinearities i.e. geometric and material.

Previous works on such analysis include the numerical procedures for approximating the failure force for zero-flexure masonry components by Sawko and Towler (1982). There have also been researches on linear elastic material properties being tested with and without flexural capacity. Romano et al. (1993) tested masonry components assuming zero flexural capacity and an average stress-strain relation for compressive loads. Such models have many shortcomings due to neglecting some characteristics of masonry materials that express their role in approximation of failure loads.

Initial tests on masonry components under axial compressive loads have depicted nonlinear stress-strain relation and a descending tail beyond the point of compressive capacity (compressive softening). In such cases, when the compressive loads go beyond compressive strength, failure of the masonry starts which is marked by the splitting of building units i.e. bricks in this case. Such analyses which are based on the assumption of masonry being no-tension material are not precise for some specific types of structural masonry work.

Parland et al. (1982) put forward a mechanism for determining buckling failure load of masonry piers, by taking into consideration tension stress field that is present in the cracked joints of such work. This study, however, also used materials of linear elastic nature. For a better analysis of such systems, it was suggested that cracking of mortar joint and the performance of mortar, as a non-linear material, should also be taken into account.

In experimental tests, lack of uniformity for testing procedures and the problems of testing stiff brittle systems results in, sometimes, contradictory data. On the other hand, in numerical methods, strange results are sometimes obtained due to the problems in monitoring cracking in a medium that is largely heterogeneous. Contact surface problems and huge analysis time also produces erroneous results.

It is, but, possible to eradicate such errors by refining the methods of modeling our problem in terms of material properties, component geometry and loading scenarios. There have been many tests on masonry components for calculating material properties but various behaviors of structural masonry are yet to be calculated with precision. Buckling and in-plane cracking are two such problems. Besides this, less knowledge is present about the interaction among several strength parameters. For instance, the exact interaction between the flexural strength of bed-joint and the factor of shearing friction at the interface of cracked joint surface is still not known.

For the components, there is a vacuum of knowledge related to different failure modes and their respective load-deformation relationships.

1.3 OBJECTIVES OF THIS STUDY

Due to the above cited reasons and the huge financial and operational demands of experimental testing of structural systems, full scale tests of structural masonry are usually less in number and limited in their interpretation of performance of such systems. Resultantly, there is scarcity of knowledge on a precise relation between experimental and numerical techniques of analyzing masonry piers and walls. The issues that need further improvement in this regard are the governing mechanisms for masonry structural components, the relationship between rigid and flexible diaphragms and their effect on structural performance, coupling effects among walls in perpendicular planes and the torsion caused due to eccentricity in center of stiffness of buildings.

This study was taken to investigate the already existing relations between experimental and numerical techniques for analysis of structural masonry and to provide an improvement in the input parameters for numerical modeling of such systems. The effect of below listed factors on the performance of masonry structures was also studied:

- effect of flexure capacity of stone/brick masonry
- material nonlinearity
- geometric nonlinearity
- eccentricity in vertical loads
- effect of support conditions on masonry structure
- mortar's nonlinear stress-strain features

This research emphasizes various input methods and parameters for numerical finite element analysis of load bearing masonry piers and walls. A 3-d finite element model was developed for this purpose. The model was subjected to different loading scenarios, including seismic loads, to approximate various strength parameters and to obtain insightful load-deformation curves, time history curves and cracking patterns.

Understandably, all of the factors of real masonry piers and walls cannot be incorporated into the analytical model but efforts have been made to ensure that the constituted numerical model fulfils maximum conditions as of the actual tested systems. Based on the comparisons, conclusions are made which highlight the effects of different parameters for use in numerical

models, characterization of damage of masonry structures under seismic loads and the effects of nonlinearity on performance of such systems.

This study focuses on the experimental, analytical and numerical finite element analysis of unreinforced masonry load bearing walls and piers. The numerical finite element model was developed, which can be approximated as being in a state of plane stress, such as panels. The walls under consideration are subjected to the vertical loads with various end condition and load eccentricity. The primary aim of this study is the evaluation of the strength and characterizes the buckling behavior of the masonry load bearing wall. The objectives of this study are:

A review on theoretical, experimental and numerical investigations of seismic failure of masonry piers and walls

- To characterize the buckling failure, develop a series of experiments of masonry load bearing piers and walls
- To select and validate a constitutive micro-model for simulating the response of the walls tested in laboratory
- To verify the developed model by comparing the predicted behavior with the behavior observed in experiments on different types of walls. The developed model should be able to predict the failure mode and the ultimate load with reasonable agreement with the experimental values
- To observe the response of wall by changing different parameters and sensitivity analysis
- To assess the accuracy and performance of available analytical formulations from masonry standards for vertical capacity of masonry walls and piers

1.4 ORGANIZATION OF THE DISSERTATION

The dissertation contains analysis of the materials features, formulation of a 3-D finite element model of masonry pier and the comparison of results of the model with that of an experimental test conducted at Earthquake Engineering Center, University of Engineering and Technology, Peshawar. The dissertation contains six chapters, outline of which is presented below:

Chapter 2 is composed of literature survey. The chapter is divided into sub-sections. Typical properties of masonry materials are presented. Failure mechanism and behavior of confined masonry buildings during past earthquake all over the world is presented.

Provisions of codes about the confined masonry buildings are discussed. The background of similitude laws is described. Finally the research work carried out elsewhere in the world on shake table and cyclic test of walls are reviewed in this chapter.

Chapter 3 presents the formulation of 3-D finite element model of a specific masonry pier. Through this chapter, various cases of input parameters for finite element modeling of such systems have been tested and their characteristics are discussed in details. The conditions for models of masonry systems with different configurations have been discussed. Values of various parameters for finite elements have also been enunciated in order to predict a better simulation of mechanical and physical features of structural masonry systems.

Chapter 4 provides details of the results of simulation of the finite element model and a detailed discussion on these results. Numerically scaled seismic excitations and the failure it causes in the subject model have been elaborated. Seismic force frequency, base shear and lateral drift have also been shown and explained in this chapter.

Chapter 5 elucidates the summary of the research work at hand. Conclusions drawn from the study are presented and recommendations are proposed in light of the drawn conclusions. Relevant potential areas for future research endeavors have also been suggested.

CHAPTER 2

LITERATURE REVIEW

2.1 GENERAL

Structural masonry is one of the oldest construction methodologies and is still preferred in most parts of the world for small to average sized residential and commercial buildings. It has the unique property to cater the demands of modern-day designs and the diverse traditional design requirements. The design criteria for masonry structures have evolved through centuries. Previously, design of structural masonry was on the lines of empirical demands of building codes for minimal thickness of walls and maximum vertical height. For columns it was based on minimum cross sectional area. Figure 1 shows a typical masonry wall panel.

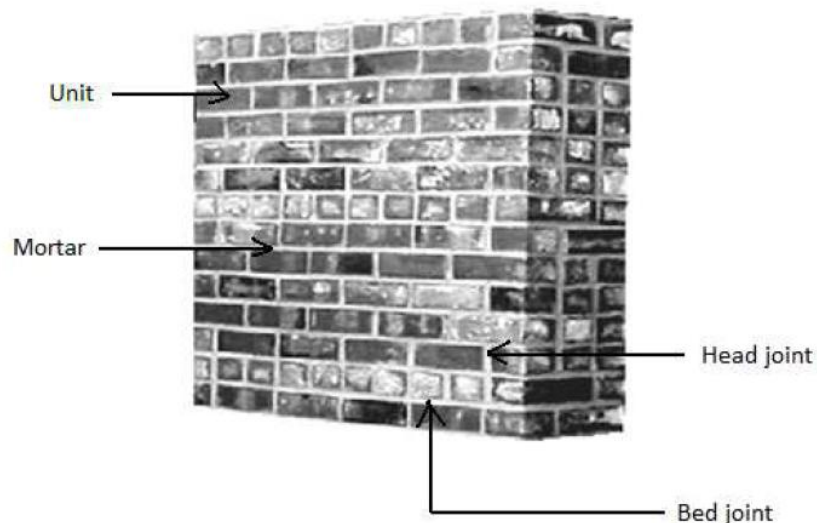


Figure 2.0 A typical masonry assemblage

It was followed by research focused on the basic components of structural masonry and unreinforced masonry elements subjected to eccentricities in loading. Research was also done on various materials that constitute masonry constructions. Subsequent sections provide some details of masonry materials.

The basic difference in masonry structures and other type of structures is the relative stiffness, combined with the configuration of elements that resist lateral forces. In masonry piers or walls, such elements are usually connected to each other orthogonally, having diaphragms of lesser flexibility. The mechanism of masonry through which it resists the lateral loads is depicted in the following figure. It can be seen from the figure that ground forces are transmitted from the footing to the walls that lay in-plane and possess a higher value of stiffness. Such load transmittal occurs in earthquakes. The transfer of these forces is smooth provided that the in-plane walls have a proper connection to the diaphragm. Table 1 shows properties of mortars.

Table 2.1. Some properties of common mortars.

| Type | Ratio (cement: lime: sand) | Compressive strength(psi) |
|------|----------------------------|----------------------------|
| M | 1:0:3 | 2500 |
| S | 0.5-1:0.25-0.5:4.5 | 1800 |
| N | 1:0.5-1.25:6 | 750 |
| O | 1:2:9 | 350 |
| K* | 0.5:2:7.5 | 75 |

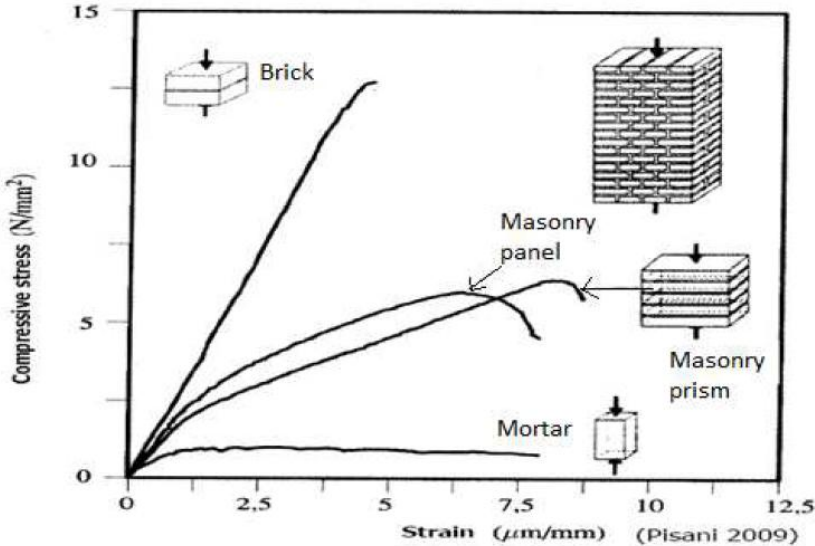


Figure 2.1. Load resisting mechanism of masonry structures

The loads are eventually transmitted to the walls that are in out-of-plane configuration. It can be observed that the mechanism of diaphragm resembles that of a deep beam with simple supports. In such cases, if the diaphragm deflects, the deflection varies with the stiffness of the subject diaphragm. In case, the masonry components have no proper connection with the diaphragm, the out-of-plane walls may separate from the diaphragm. This causes the out-of-plane walls to undergo independent vibrations and hence, increase the seismic proneness of the entire building. Figure shows behavior of masonry structure subjected to lateral loads for different kinds of wall-floor connection and different types of floor-slab configurations.

2.2 SEISMIC PERFORMANCE EVALUATION OF UNREINFORCED MASONRY BUILDINGS

Previously, different approaches have been utilized to judge the seismic response of unreinforced masonry, numerically and experimentally. As of now, a total of 33 major experimental investigations have been carried out around the globe, to evaluate unreinforced masonry components, with emphasis being on piers and walls.

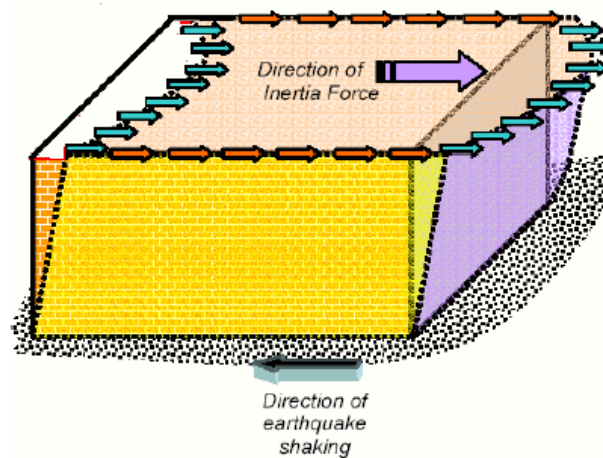


Figure 2.2. Reaction of masonry to seismic loads

This includes the work of Epperson and Abrams (1989), Magenes and Calvi (1992), Abrams and Shah (1992), Manzouri et al. (1995), Craig et al. (2002), Anthoine et al. (1995), Franklin et al. (2003). For Pakistan, Kashmir Earthquake of 2005 started a series of experiments on masonry

buildings and components. Experimental tests have been performed by M. Ashraf (2010), A. Naseer (2010) and M. Javed (2009). Q. Ali (2004), in his research, subjected a full scale single room masonry assemblage to ground motions through a controlled sub-surface explosion. A couple of other full scale tests have also been performed in different parts of the world but the results cannot be applied to evaluate all types of masonry works, especially the kind of stone and brick masonry structures that are found in Pakistan. Figure 3 shows masonry reaction to earthquake.

Table 2.2 Reaction of different form of masonry structures to seismic loads

| Design ground acceleration | | < 0.2 g | 0.2-0.3 g | ≥ 0.3 g |
|----------------------------|------------------|-------------|-------------|-------------|
| Unreinforced Masonry | Height, ft (m) | 39.4 (12.0) | 29.5 (9.0) | 20.0 (6.0) |
| | No of stories, n | 4 | 3 | 2 |
| Confined Masonry | Height, ft (m) | 59.0 (18.0) | 49.0 (15.0) | 39.5 (12.0) |
| | No of stories, n | 6 | 5 | 4 |
| Reinforced Masonry | Height, ft (m) | 79.0 (24.0) | 69.0 (21.0) | 59.0 (18.0) |
| | No of stories, n | 8 | 7 | 6 |

Different types of structures used different type of materials and employ different construction techniques. This study was, therefore, focused on typical unreinforced stone and brick masonry

2.3 IN-PLANE FAILURE MODES IN UNREINFORCED MASONRY WALLS

The complexity in the behavior of masonry structures is mainly due to the large non-homogeneity and the anisotropic composition of masonry building blocks. The exact and accurate calculation of lateral force capacity of ordinary masonry components is complex because of the intricate relations between mortar and stones or bricks. There exist some failure theories that can predict the failure mechanism of a specific structure for a specific condition of generated stresses. Additionally, some analytical models are also proposed which can possibly approximate the capacity of masonry structures. Some of the models are detailed in the subsequent sections.

2.4 TOE CRUSHING/ROCKING FAILURE MODE IN URM WALLS

Failure starts at the moment when tension cracks start to originate at the top and bottom of a tested masonry column. Increasing the displacement causes the pier to deform like a rigid body and it start to rotate around the toe that is compressed. Crushing of toe can be summarized as a compressive failure that occurs at the bottom end of a pier i.e. toe of a pier. Such times of failures can be observed in piers that posses large aspect ratio and are subjected to compressive stresses of medium to high value. If no rocking failure takes place, then crushing failure can be of brittle nature. Following figure presents the rocking failure mechanism of masonry piers and depicts the failure through crushing at the toe.

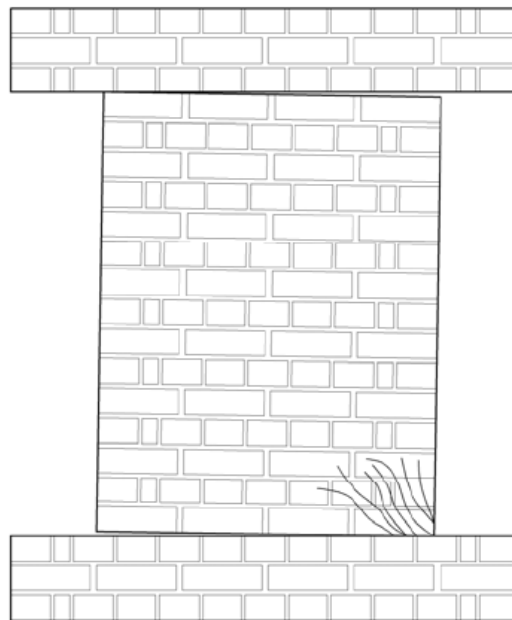


Figure 2.3. Toe crushing failure

The capacity of such piers to resist lateral loads can be calculated by employing the equation given by Magenes. Lateral capacity of pier corresponding to this failure mode is determined by using the equation (Magenes and Calvi 1997).

2.5 SLIDING SHEAR FAILURE MODE IN URM WALLS

Sliding shear failure is observed in those piers which have a low aspect ratio and are subjected to lower compressive loads. Such type of failure is usually ductile in nature and reasonable energy is dissipated because of wall's sliding around a separated joint of mortar. This type of failure causes lesser damage to the pier; following figure shows a sliding shear failure in a masonry column. Usually, the criterion given by Coulomb is employed to calculate damage of such nature (Magenes and Calvi 1997).

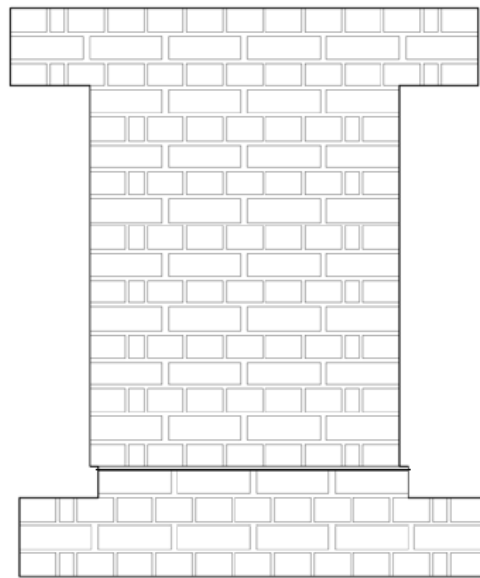


Figure 2.4. Sliding Shear Failure

This criterion was further extended to derive a relation for estimating the sliding shear force and hence develop an equation for this purpose.

2.6 DIAGONAL TENSION SHEAR FAILURE MODE IN URM WALLS

Diagonal flexural cracks usually originate at the middle of columns with around 45 degrees slope. The direction of their propagation depends upon the difference between strengths of mortar and the building bricks or stones. If the bricks/stones are weak the crack propagates through the bricks as shown in following figures. On the other hand, if the mortar is weaker than

the bricks the crack propagates through the mortar as can be seen in the below given figure. Such kind of failure is of brittle nature and results in sudden loss of strength and total stiffness of the structure. Diagonal flexural failure usually happens in piers having low aspect ratio, subjected to high compressive loads. In such cases the lateral load resisting capacity of piers can be estimated through the equation given by Turnsek and Sheppard (1980).

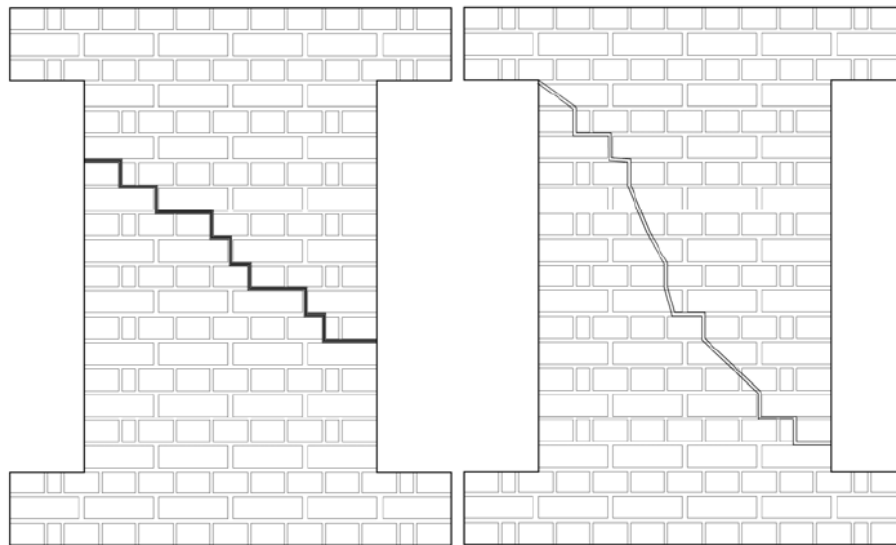


Figure 2.5. Diagonal flexural failure

As per the code of FEMA 307, the drift is estimated for various failure mechanisms as given by Simsir (Simsir 2004). The drift capacity of column will be approximately 0.50% in case the column/pier is failing due to diagonal flexure or due to crushing of toe without sliding. The ultimate drift has a range of 1% to 2% in case the failure of pier is sliding (or rocking) prior to failure due to diagonal or crushing of toe. The elastic stiffness of masonry column K_e is estimated by equation 274 of FEMA. It is derived while taking into account shear and flexural deformations.

2.7 CONFINED MASONRY

Confined masonry is largely present in Latin America, Europe and Asia. In such type of masonry construction, vertical and horizontal confining components are used to confine the masonry walls as shown in the figures given below. The horizontal and vertical confining components enhance

the ductility of the buildings and as such also increase its seismic performance. Resultantly, it adds to avoiding the disintegration of walls in case of earthquakes and other lateral forces. As the horizontal confining elements tie together the walls, they are, therefore, also known as bond beams. For such systems, the masonry walls are erected first and later concreting is done at location of columns and beams. The contribution of such confining components must be considered while computing the lateral resistance of such buildings (Eurocode6 and Eurocode8).

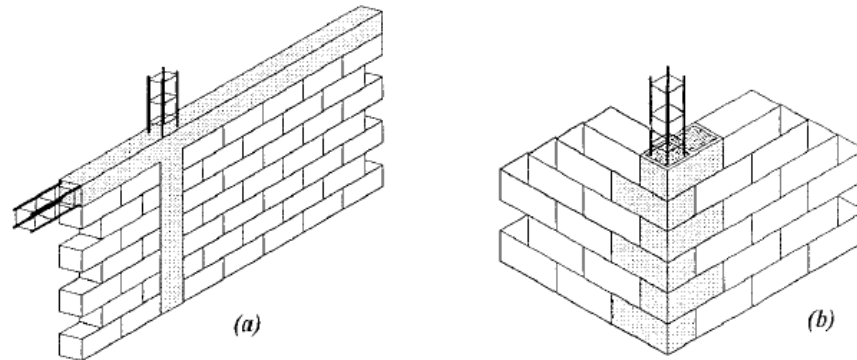


Figure 2.6. Typical confined masonry

2.8 PLANE FAILURE OF CONFINED MASONRY BUILDINGS

Flexural failure, sliding failure and diagonal shear failure are the various kinds of in-plane failures that can occur in confined masonry structures.

Horizontal in-plane loads of inertia are transmitted in such buildings by diagonal strut as presented below, from the upper floor to lower floor and subsequently to the footing. Diagonal cracks are originated in the confined masonry structures when the diagonal flexural stresses due to diagonal compression loads go beyond the diagonal flexure strength of the binding mortar. Different factors governing this failure are low flexural strength of mortar and brick-mortar bond strength (Naseer 2009).

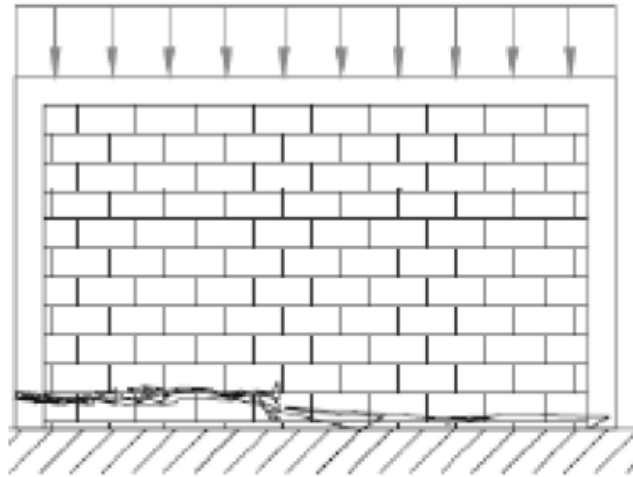


Figure 2.7. Cracking in confined masonry under monotonic gravity loads

Diagonal shear cracks originate and propagate into the tie pier, hence cracking the pier. When the stress demand is increased, it can be observed that crushing of concrete takes place in the tie pier and crushing of bricks takes place in the middle of the walls (Tomazevic, M., 1997; Ishibashi, K., et al. 1992). It is known from the past earthquakes and from experimental studies that the concentration of diagonal cracks takes place in the ground floor (Alcocer et al., 2004)

The other type of failure in confined masonry structures is sliding shearing of in-plane walls. Such kind of failure mainly takes place in horizontal direction due to failure of brick-mortar bond in shear. Third type of failure in confined masonry structures is failure in tension. In such cases, horizontal cracks develop in walls when the flexural stresses go beyond the flexural strength of mortar. This is shown in the above figure.

2.8 CONNECTION FAILURE

Various types of failures of connection are the separation of masonry structures from confining components or other masonry components. This includes separation of masonry wall and bond beam and failure of connection between vertical and horizontal confining component. The failure of such joints alters the failure mechanism of the entire structure. The masonry components i.e. walls no longer transmits the flexural stresses to vertical confining components, effectively.

1. The separation between vertical confinement element and the masonry wall will cause high in-plane or out-of-plane stresses. In-plane performance is affected as the transfer of tensile stresses from masonry (walls) to concrete (pier) is not effective. As the masonry structures are not supported by the confining components, the out-of-plane response is also affected. This type of connection failure between pier and wall has been observed in masonry structures subjected to earthquake loads.
2. The other type of connection failure is also caused by in-plane or out-of-plane excessive loading. The failure shows its effect by weakening out-of-plane capacity and by reducing the in-plane load transmittal. This causes cracks at the joints between floor slabs and walls.

2.9 SEISMIC DAMAGE ASSESSMENT

In Japanese building Code, the following Procedure Route is employed to assess the seismic damage of small structures with height less than or equal to 20m. Seismic damage has a relation with wall density ratio of a structure (Shiga Toshio, 1978) and can be calculated from the equation given by them.

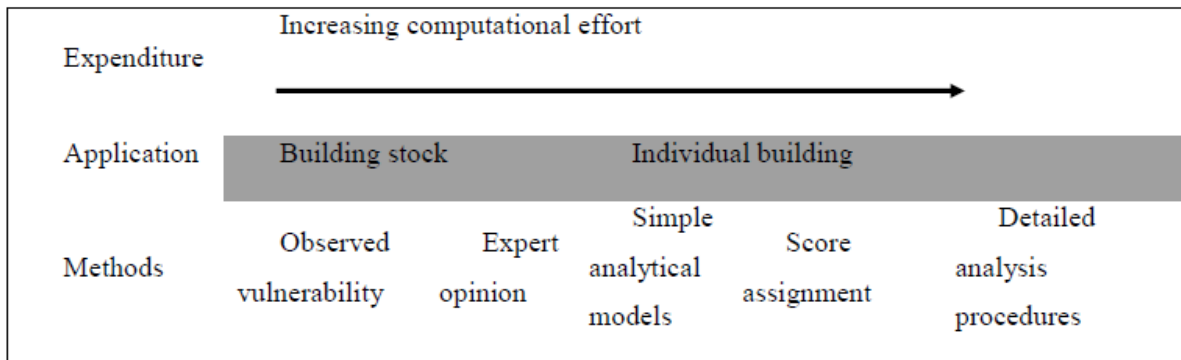
2.10 SEISMIC VULNERABILITY ASSESSMENT OF BUILDINGS

Seismic response of an isolated structure can be conveniently investigated by experiments. But it is impossible to estimate the seismic capacity of the entire building stock of a locality and neither is it possible to characterize the seismic damage of all the buildings in a given city. For evaluating the seismic response of the building stock of a given locality/city, seismic risk assessment is conducted by exploring the seismic hazard of the area and seismic vulnerability evaluation of structures of that area. Seismic hazard is based upon the geology of an area and the distance of that locality from active seismic sources i.e. faults. Structural systems, constituent materials and mechanical properties, geometry of structures and configuration of floor-wall joints are some of the factors that affect the seismic vulnerability of a given structure.

A vulnerability assessment method was given by S.W.Cochrane and W.H.Schaad in 1992 which was based upon different features of structures e.g. building age, regularity and symmetry, usage, subsoil condition, height of structure and material properties (Cochrane and Schaad 1992). Following are the steps for assessment of seismic vulnerability of buildings:

1. Gather data regarding the characteristics of building that would possible affect its vulnerability.
2. Compose vulnerability assessment tools which will encounter the features of buildings of a given locality.
3. Different methods for assessment of seismic vulnerability of structures are given in the subsequent sections of this dissertation. Lang (Lang 2002) had detailed the procedure for such vulnerability assessment. Different approaches that can be employed for assessing seismic vulnerability of buildings are given in below stated Table.

Table 2.3 Flow chart of seismic vulnerability assessment



2.11 OBSERVED VULNERABILITY

Observed damage characterization is primarily obtained from statistical data acquired from damage to buildings in past earthquakes. This method is very raw and suitable only to structures that are non-engineered and the numerical or experimental assessment of which is difficult and costly. Such investigations were first conducted by Whitman for studying effects of San Fernando Earthquake of 1971 on structures. He gathered the damage data of about 1500 affected structures and formulated damage probability matrices (DPM). Such matrices have the ability to

give the probability of occurrence of various stress levels of different intensities. Other studies of same kind were conducted by Poro (Poro et al. 1989).

This approach has many drawbacks as it requires inventory data of many structures. This method also does not propose retrofitting of buildings for reduction of vulnerability.

2.12 EXPERT OPINIONS BASED SEISMIC DAMAGE ASSESSMENT

First expert opinion based damage characterization approach was carried out in a FEMA sponsored project that was conducted at Applied Technology Council. In the said document, Damage Probability Matrices were made for 78 earthquakes. 58 experts were interviewed to assess the damage of particular structural system subjected to action of various intensities of earthquakes. A specified proforma with questions regarding the effect of earthquake on building was being filled by all the interviewers. Following this study, many versions of this procedure were put forward by many researchers (Kircher et al. 97, Pujades et al. 2000). The main disadvantage of this method is the difference in personal opinion of the interviewers, based on their knowledge and experience. Similarly, this was basically a case study and the results cannot be applied for other types of buildings in other localities. Also, this method cannot be applied to those areas which do not have experienced earthquake in the past as no data was available for them.

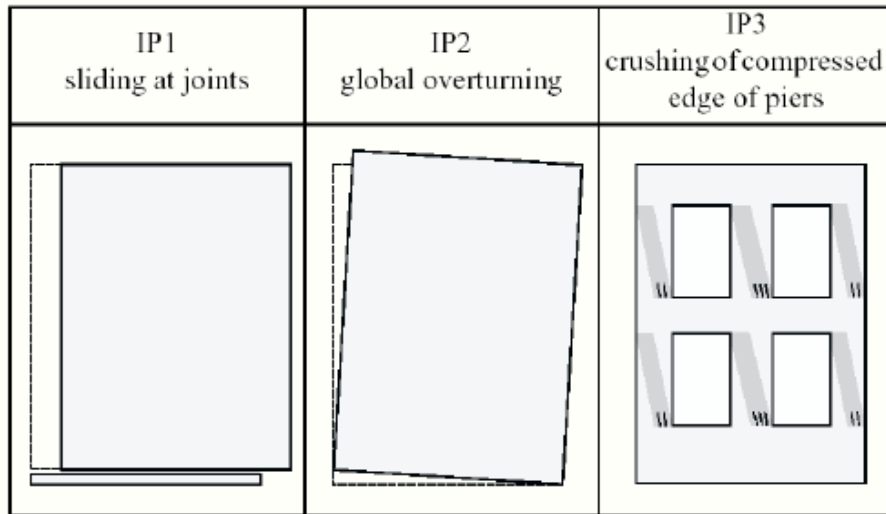
2.13 SIMPLE ANALYTICAL MODELS BASED EVALUATION OF DAMAGE TO MASONRY BUILDINGS

This approach can be applied to areas that have not experienced earthquakes in the past. Also this method can assess many buildings in much lesser time than the other two forms of damage assessment. Its efficiency can be improved if the input parameter for analysis can cover the entire seismic response of the structures. For towns of Europe, an analytical approach was formulated and tested for assessment of buildings (Ayala et al. 97).

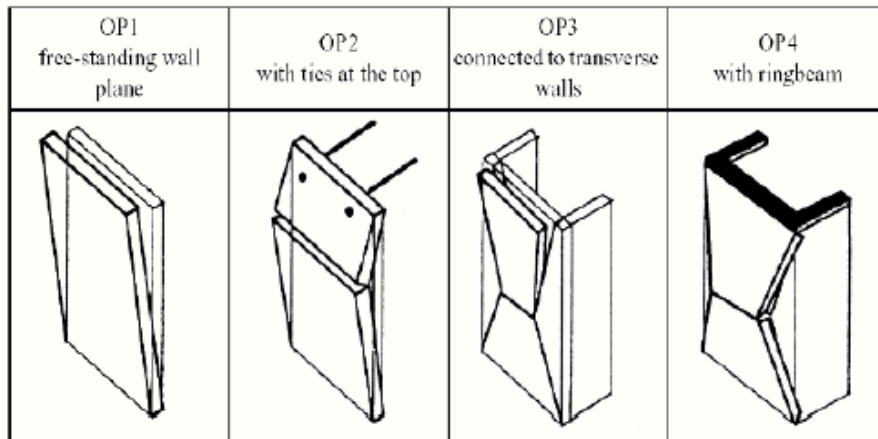
This method was then tested for Alfama District of Portugal and for the villages that were struck by the Umbria-Marche earthquake of 1997 (Spence et al. 99). In-plane and out-of-plane failure

models were considered for this specific case. The anticipated collapse mode and capacity of structures are estimated through visual observations of boundary conditions and the geometry of structure.

There are two further classifications of the in-plane and out-of-plane failure modes. They are shown in the following figure . Each failure mechanism is connected to a damage scale as per the European Macroseismic Scale (EMS 1998).



(a)



(b)

Figure 2.8. (a) Overturning failure (b) Connection failure

Calve put forward a displacement-based method for damage evaluation of structures and was first applied for structures in Catania City (Calvi 1999). The main advantage is that it can be applied for both i.e. masonry structures as well as concrete structures.

Out-of-plane failure is neglected and only in-plane failure is taken into consideration in this type of damage assessment. Lesser number of factors is taken into account for this model i.e. number of floors, age of structure and construction material properties.

This analytical approach has the advantage of many buildings in lesser time but its precision is affected by the crude assumptions made for simplification.

2.14 ADVANCED CAPACITY SPECTRUM METHOD

Different structural systems require different structural analysis approaches and each, subsequently, requires a different representation of ground motions during earthquakes. In equivalent linear analysis method, spectral accelerations of certain periods are required to calculate seismic loading. While on the other hand, in the spectral analysis approach, spectral earthquake demand is needed.

For some of the improved capacity spectrum methods, time histories are required. The demand spectrum is of importance in the assessment for Advanced Capacity Spectrum Method.

Linear as well as non linear history analysis utilized earthquake records and is preferred in most cases due to their precise representation of ground motion parameters e.g. duration of motion and the time-dependant amplitude.

The ACSM also helps to cater for the difficulties that are present in nonlinear static analysis and provided improved calculation of structural performance and damage.

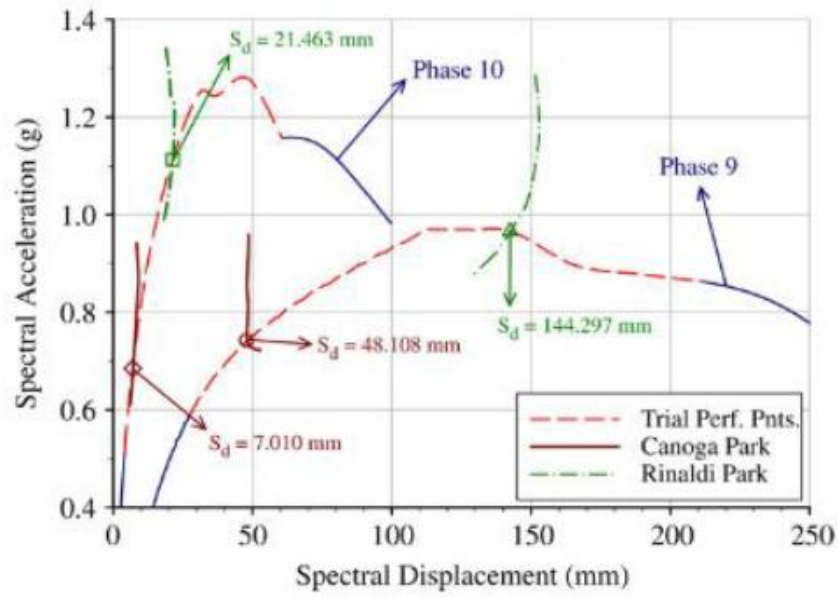


Figure 2.9. Spectral displacement in masonry structures

CHAPTER 3

EXPERIMENTAL AND NUMERICAL TECHNIQUES FOR SEISMIC DAMAGE EVALUATION OF UNREINFORCED STONE AND BRICK MASONRY STRUCTURES

3.1 GENERAL

Many experimental and analytical techniques have been employed by researchers to evaluate the seismic response of masonry structures and to characterize the damage caused thereby. Some of the experimental methods are quasi-static (slowly reversed cyclic) loading, monotonic static loading, dynamic testing by use of shaking tables (earthquake simulator) and pseudo-dynamic tests. Other methods include impact table testing and excitation of subsoil by controlled explosions. Numerical methods comprised of heterogeneous and homogeneous modeling by use of discrete element models, finite element models and interface components.

Below is a brief account of some of the experimental and numerical methods.

3.2 STATIC MONOTONIC AND QUASI-STATIC LOADING

In such type of monotonic loading method, the static load is subjected in single direction only while in quasi-static load application; the structure is subjected to loading cycles of force or displacement of predefined amplitude until the point when failure of the structure happens. The facility of static monotonic loading present at the University of Engineering and Technology, Peshawar is presented in the following figure.

A recent research that involved the simulation of seismic response by application of various displacement patterns showed that if different deformation patterns are employed for testing equal masonry wall models, there might be much difference in results. As the variation in results goes beyond the normal scattering of quality of structures of masonry, it is of significance that testing procedures for evaluating the seismic response should represent the actual seismic behavior of masonry structures.

With the advent of strong, computer monitored hydraulic actuators, larger and powerful high performance seismic simulators (HPSS), research personnel recently have preferred pseudo-dynamic and shake table testing for studying the damage of masonry structures.

3.3 DYNAMIC TESTS USING SHAKES TABLE

In such approach, the subject structure is firmly anchored on a shake table. Computer controlled hydraulic actuators that have the ability to simulate earthquake events vibrate the table in a given direction. This is recently the only method that could simulate real ground motion events for assessing damage and seismic capacity of structures. large shake tables having dimensions of 8m x 8m, with six degrees of freedom shaking and having capacity of simulating earthquake motions of displacements of +/- 600mm and having velocities of 2m/s are presently available and in use. A 100-ton specimen can be tested for an acceleration of 2g. For reduced accelerations, specimens up to 300 tons can also be experimentally tested as shown in the following figures.



Figure 3.1 Model being tested on shake table



Figure 3.2 A typical shake table with hydraulic actuators

3.4 PSEUDO-DYNAMIC METHOD

The schematic setup of pseudo-dynamic method is illustrated in the below given figure. For such a setup the kinematics of the specimen structure are supposed to be well reflected by a particular number of degrees of freedom e.g. the horizontal deformations at each slab floor level. A recorded earthquake ground motion data is fed to the computer. For the first time step, the horizontal deformations of floors are computer by numerical integration of dynamic equation of motions. For this purpose inertial forces and viscous forces are modeled through analytical methods (such as matrices M and C). These deformations/displacements are then fed to the structure by hydraulically controlled actuators that are connected to a strong wall or reaction wall. Load-cells mounted on the actuator give a measurement of the forces necessary to obtain the demanded deformation. These forces are then employed for the following time step for computing the next displacement and the cycle goes on until the structure fails.

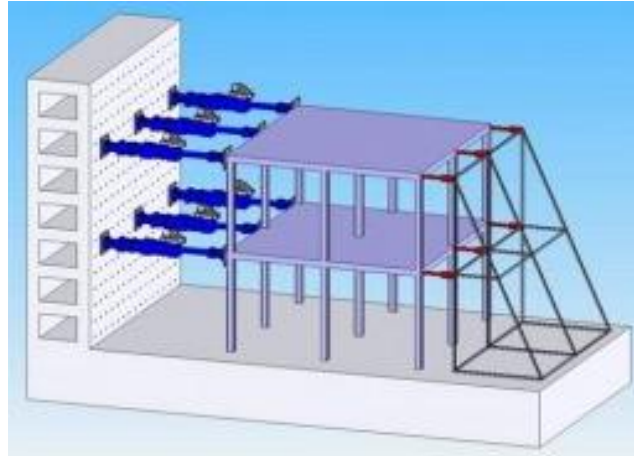


Figure 3.3. Setup for pseudo dynamic testing

Because of the analytical representation of initial forces, there is no requirement for performing the test on a real time scale. Usually an earthquake event of ten seconds is applied to a structure pseudo-dynamically in one hour approximately. This is one of the major merits of the pseudo-dynamic methods which is not present in shake table testing. Pseudo-dynamic testing allows for a detailed monitoring of the propagation of damage in the structure for given applied loading. Another advantage is that pseudo-dynamic test can be halted at any moment for examination and marking of the damage caused by the forces applied until that level.

Also, with pseudo-dynamic testing methods, large structures can be tested which cannot be conveniently tested with other methods such as shake table testing.

3.5 FINDINGS FROM PREVIOUS TESTS CARRIED OUT ON MASONRY STRUCTURES

Most of the research experiments for seismic damage assessment of masonry structures used shake table tests and pseudo dynamic tests. There are a few quasi-static tests whose results are available for study.

Some of the important tests regarding such studies are given in the subsequent sections.

3.6 SHAKING TABLE INVESTIGATION OF MASONRY HOUSES, UNIVERSITY OF CALIFORNIA, BERKELEY USA

When the UBC altered its zonation map, Phoenix, Arizona was included in zone 2 instead of zone 1. The Department of Housing and Urban Development (HUD) California suggested that masonry structures in phoenix must be partially retrofitted. There was concern raised about this alteration in construction requirements due to non-availability of evidence for such increased earthquake resistance of masonry houses in that area. A project was, therefore, undertaken at UCB for the evaluation of seismic behavior of masonry structures. This project was mainly focused on determining the maximum earthquake force that the unreinforced/un-retrofitted masonry structures could tolerate without significant damage.

The advantage of this study was the full scale testing of elements of masonry houses on a shake table of two components, i.e. horizontal and vertical acceleration Masonry wall panels were fabricated of commercially available concrete units or clay bricks. The specimens were then subjected to different base motions of varying intensity. El Centro 1940, Pacoima 1971 and Taft 1952 were the three earthquakes that were simulated for this study. Response of the structures was measured and recorded with the help of a large number of sensors and transducers.

Important findings of the study are as follows.

1. It was observed that typical masonry houses have enough rigidity to not create a very complicated dynamic response mode during an earthquake event. The response of tested houses was in close agreement with the shaking table response. Distortions and deformations were mainly in-phase with the base excitations. It was thus inferred that frequency features of earthquakes are not major factors for causing seismic damage in masonry structures. It was instead the peak value of acceleration of ground motion that predominantly quantifies the damage by earthquakes.
2. Very less or no cracks were seen in major wall panels tested for peak acceleration values lesser than 0.2g. The lowest value of peak acceleration of ground that caused development of cracks in non-bearing walls was 0.21g. It was thus declared as the minimum intensity to bring about cracking of out-of-plane wall panel.

3. Out-of-plane masonry walls performed satisfactorily cracks appeared at increased intensity. Displacements of such walls became larger for tests that were performed with peak accelerations above 0.4g. These large deformations caused hinging at crack interface and showed the structure was unstable. There was, however, no actual collapse in any test.
4. The amplification factor at top end of masonry wall is between 1.0 and 1.5.
5. The study suggested that for a PG value of 0.1g, the minimum span length of element encountering shear should be 6ft. for a PGA value of 0.2g, the minimum length of such an element should be not less than 9ft. Elements that are bound to resist shear, i.e. Masonry walls, must extend from floor to slab of that storey without any discontinuity.

3.7 MASONRY WALLS SUBJECTED TO SHAKE TABLE TESTING; UNIVERSITY OF PAVIA, ITALY

In order to test the influence of mortar strength, axial load level and aspect ratio on the dynamic behavior of brick masonry walls, shake table test were performed on such specimens. The results for the above mentioned parameters helped in formulation of various failure modes with better seismic response or unfavorable response.

Findings of this study are listed below.

1. Higher axial loads and lower aspect ratios calls for diagonal cracking of specimens whereas with lower axial loads and slender wall panels, sliding and rocking failure have more tendencies to occur.
2. Shear failure is observed (unfavorable) and no rocking failure is seen (favorable) when higher strength mortars are used for specimen testing.
3. The transfer from a favorable failure mode to an unfavorable failure mode is a masonry wall panel was obtained by taking the axial load level towards higher values.

It was, thus, concluded that:

1. If mortar strengths is more than demanded, it can cause brittle failure which is not favorable.
2. Axial loads of too high or too low values can cause unfavorable results.

3.8 MASONRY AND ADOBE HOUSES SUBJECTED TO SHAKE TABLE TESTS; STANFORD UNIVERSITY CALIFORNIA, USA.

This study was taken at the Stanford University for evaluating the feasibility of various techniques for experimentally assessing the seismic damage of single storey masonry structures. The material in this study was adobe, low strength bricks and unfired brick units. The researchers of this study explained in depth the difficulties in dynamic modeling in reduced sized models for a shake table facility. After studying the properties of such masonry structures in detail, the authors agreed that neither shake table testing nor pseudo-dynamic testing can properly reflect the seismic performance of unrefined masonry structures.

3.9 CORRELATION BETWEEN DYNAMIC AND STATIC BEHAVIOR OF MASONRY STRUCTURE; UNIVERSITY OF ILLINOIS AT URBANA-CHAMPAIGN, USA

The subject research study was part of a US-Japan Masonry Research Project and it details the correlations among responses of a give structural system subjected to both i.e. static lateral loading and dynamic shake table testing.

Tow model structures were constructed with same designs criteria and were tested using two completely different methods. The first other specimen was subjected to simulated earthquake ground motions through a shake table whereas the second model structure was subjected to displacement through computer controlled hydraulic jacks. The same time history was maintained for both the tests. Relations were constituted between the responses of the dynamically and statically tested model structures. Comparisons were drawn to propose differences in energy dissipation, total stiffness and strength of the structures that may be caused with wither of the testing methodology.

Following conclusions were drawn from this study.

1. The shake table tested models structure showed more endurance for dynamic forces than the one tested through static loads. Degradation in stiffness and strength were comparatively more for the static specimens. Damage was also observed to be more in the model tested for static forces.
2. If the deformation resistance is not contained for the dynamic shake table testing, static laboratory experiments suggest a conservative method for computing response of actual masonry assemblages subjected to earthquakes.

It has been previously discussed in the preceding sections that static method for assessing the seismic damage and dynamic characteristics of structures can cause errors in results. However, in absence of other viable alternatives, the static method can be employed for a conservative testing technique of actual masonry structures.

3.10 EXPERIMENTAL INVESTIGATIONS ON BEHAVIOR OF UN-REINFORCED MASONRY WALLS UNDER SEISMICALLY INDUCED LOADS; INSTITUTE FUR MASSIVBAU, GERMANY

In this research endeavor quasi-static tests and shake table tests were conducted to characterize the fundamental response of masonry walls when subjected to shearing in-plane cyclic loading. Wall panels with dimensions of $L/H/T = 1.24/1.24/0.115$ meters were tested on the earthquake simulation equipment installed at Institute Fur Massivbau, Germany. A base acceleration time history that was recorded for the Friuli earthquake (1976) was used for this study. In steps the model structures were loaded with various numbers of base excitations of increasing magnitudes. For a more detailed assessment of seismic damage, quasi-static tests were also carried out. Different values of axial loadings were applied for investigating the different failure patterns.

Results of the tests can be summarized as follows.

1. Under low axial forces, cracking propagates through the mortar joints along the diagonally placed units. When axial load was increased, straight diagonal cracker were produced which broke into the unit i.e. bricks in this case.

2. In cases which depicted primarily cracking of the mortar connections only, a considerable amount of plastic deformations was seen. The isolated portions of the wall panels, being separated by such cracks, slid past on adjacent portions and caused large deformations. The deterioration of strength was meager because the strength capacity was mainly dictated by frictional resistance, which did not change. When building unit cracking was dominant, the individual wall sections between cracks were not unstable and slide along the diagonal crack interface. This type of failure is brittle and was more dominant with increased values of axial loads and finally resulted in brittle failure which was explosive in nature and showed no or less plastic deformations.

3.11 MASONRY MATERIALS AND PROPERTIES

As it is known that masonry is a composite material which comprises of building units and binding mortars. Due to the variation in the properties of the units and mortars, the overall properties of masonry vary over a large range. For instance the most common mortar is made up of cement, sand and water. But other types of mortars are also present in the field and are widely used for masonry works. In the following sections different types of mortars that are presently in use in field of masonry construction will be discussed.

Concrete blocks, clay bricks, clay tiles and dressed stone have been used worldwide as masonry building units. Stone masonry is focused in this research study because of its wide presence and it's used in historical constructions that are seismically vulnerable.

The composite mechanical properties of masonry are a function of the combined mechanical properties of the constituent materials and the bond between them. Generally, unreinforced stone masonry structures are anisotropic in nature. It is but for reasons of convenience that elastic features of masonry units are taken as isotropic.

The elastic properties of masonry units, while considering them isotropic, are taken from the data of the vast number of experimental results on masonry prisms. The cumulative elastic modulus of masonry is governed by the combined modulus of elasticity of masonry units and the binding mortar (Hamid et al. 1987). Past research studies show large scattering in the results obtained for elastic modulus of a masonry assemblage. These can be attributed to two main reasons. Firstly,

the properties of masonry building units and those of the binding mortar themselves vary largely when different combinations of materials are used for mortars or different form of masonry units are utilized. Secondly, there always is a difference in the degree of quality of workmanship while constructing masonry structures.

There exists an equation given by the European Code (EC6 1995) for computing modulus of elasticity and shear modulus of a masonry structure.

Other researchers are of the opinion that stone and brick masonry is actually a nonlinear material and therefore, its elastic modulus is different at different values of stresses. A typical stress-strain relationship of stone, mortar and masonry prism is shown in following figures. Normally the cumulative compressive strength of masonry is somewhere in between that of the mortar and the stone or brick. Compressive strength experiments are relatively easy to carry out and it illustrates a good idea of the overall quality of the comprising material(s). The Eurocode 6 (1995) agrees on the compressive strength of the masonry components to indicate the overall strength of the masonry even if the exact values of those parameters are not precisely known.

3.12 BUCKLING AND MATERIAL OVERSTRESSING

Most of the compression members normally fail due to buckling which is primarily caused by material overstressing. Slender members are more prone to buckling. Graphical representation of buckling failure is shown in below given Figure. The figure illustrates that as the reduction factor and the slenderness ratio of compression member increase, the chances of its buckling failure increases. Material failure happens when slenderness ratio is low and reduction factor is high.

In cases where slenderness ratio is high and reduction factor is low the predominant failure is that of buckling. In cases with lower slenderness ratio and higher values of reduction factors, there are more chances of Euler buckling.

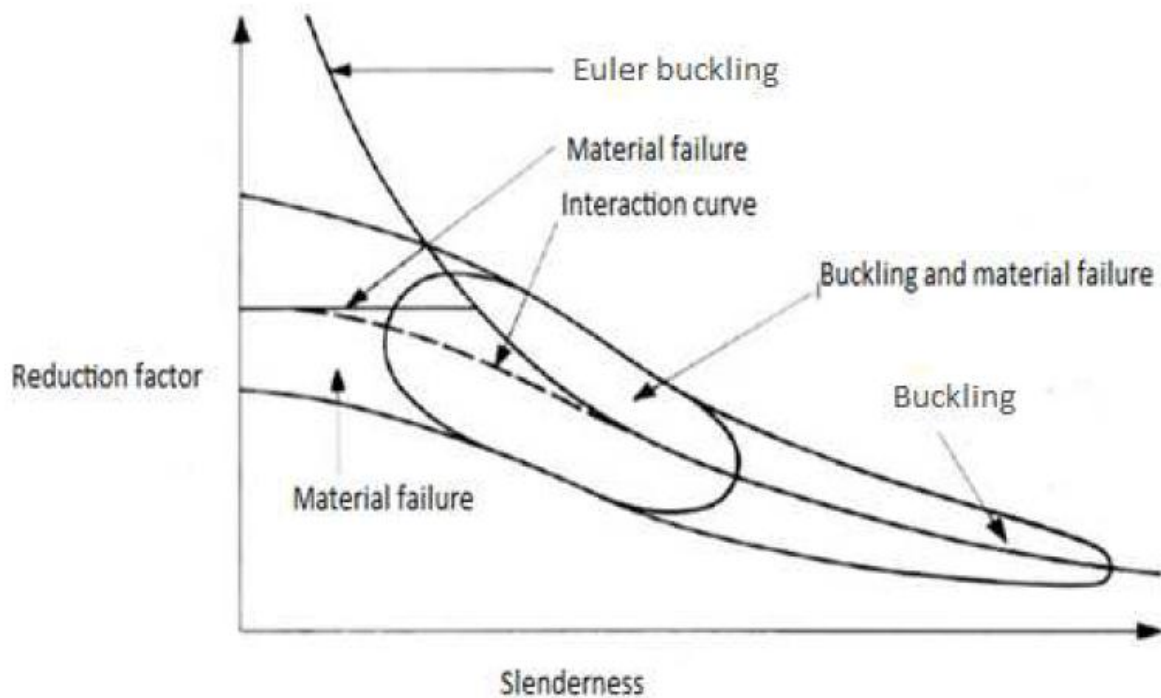


Figure 3.4 Graphical representation of buckling of masonry piers and walls

The mathematical equation derived by assumption of an ideal strut and given by Euler is an empirical one and is a part of Eurocode 6.

3.13 ANALYTICAL AND NUMERICAL APPROACHES

Yokel (1971) successfully developed an analytical relation to calculate the critical load for prismatic members which have cracked sections mainly cause by low tensile capacity of the section. The research was carried out for a prismatic rectangular element, made up of an elastic material and the stress-strain relationship of the material was linear. The loading combination applied by Yokel comprised by a load P acting in an orientation parallel to the element's axis. The load was applied by maintaining an eccentricity of $t/2 > e > t/6$. Support conditions at both ends were assumed to be hinged, thus, providing no restriction to rotation as shown.

Cracks started to appear on the flexure side of the cross section because of no or very less tensile strength of the material. The un-cracked portion of the element has a stress distribution as shown

in contour plot below. Stress distribution throughout the body of the wall is presented in below stated figures.

The distance u , which is the distance between the line of action of force P and the compression face, varies with the height of the element.

This is due to the deflection of the member. A maximum value of this distance is obtained at the two ends of the member. Understandably, the minimum distance is at the mid-height of the member.

Many significant advances have been made in masonry applications in recent past. As discussed in earlier sections that masonry is a composite construction material, hence it requires special attention for its finite element modeling.

Generally two types of modeling techniques are used for modeling masonry structures i.e. micro-modeling technique and macro-modeling technique. Micro-modeling technique suits well when small structures are under study where the prime interest is in the heterogeneity in stress and strain.

On the other hand, macro-modeling is good for analysis of large structures and is common for industrial usage.

3.14 SOFTENING BEHAVIOR OF MASONRY

It is gradual degradation in the mechanical resistance due to continuous increase in the deformation that a material sample or structure specimen is subjected to. This characteristic is generally found in materials like ceramics, fired clay bricks, cement-sand mortars. Such materials are quasi-brittle in nature and they fail mainly because of propagation of internal cracks.

This type of behavior of materials/structures is generally caused by large heterogeneities in them. Research has shown that even before loading, mortar has hairline cracks due to shrinkage and due to the transition boundaries of aggregates.

CHAPTER 4

NUMERICAL REPRESENTATION THROUGH FINITE ELEMENT MODELING FOR DAMAGE STUDIES OF MASONRY STRUCTURES

4.1 INTRODUCTION

Compared to macro-modeling approach, the micro-modeling approach is considered as a more accurate technique to assess the seismic analysis of masonry structures and has been use in this very case for study. Micro-modeling allows a proper simulation of the response of masonry by considering joint flexural cracking and the crushing of masonry in compression. In this case, the estimation of the ultimate strength of masonry piers is calculated through micro-modeling method. Previous results from masonry modeling standards are also taken into account and are compared with this work's data.

In this study, special attention is given to the seismic load bearing wall tests carried out in the UPC (2009), because most of the parameters necessary to characterize the material model are available from micro-experiments. The main concern of this work was, to demonstrate the ability of the model to capture the behavior observed in the experiments and close quantitative reproduction of the experimental results.

For the numerical analyses, units are represented by plane stress continuum elements (8-noded) while line interface elements (6 12×3 elements).

4.2 ADOPTED MODELING STRATEGY

The numerical simulation presented is performed with the well-known micro-model proposed by Lourenco & Rots (1997) requires more specific software oriented to masonry analysis. For all cases, micro-models assume 2D plain-stress and a hinged-hinged configuration. The hinges are modeled by means of stiff triangular objects placed at the bottom and at top of the wall, whose end vertex is allowed to freely rotate. In addition, a minimum eccentricity of 1mm is always applied in order to account for possible irregularities of the wall geometry of the load

positioning. Basically, the model assigns an elastic behavior to the units whereas masonry inelastic behavior is transferred to the joints. This analysis was performed with ANSYS software.

There are two broad classifications of numerical models for masonry structures. They are homogenous models and heterogeneous models. Homogenous models are fabricated by keeping in view the assumption that masonry is a continuum material. The properties for masonry in this case either acquired from tests or obtained from empirical equations. Heterogeneous models are those which analyze masonry systems by discretizing the building units and mortar individually through finite elements. In studies where masonry structures are subjected to seismic excitations, both homogenous and heterogeneous models are used. These models are analyzed by dynamic analysis methods. Bricks are usually taken as solid elements and interface mortar is modeled as shell finite element. 3-D models are preferred and linear elastic solutions are mostly run on the models with cyclic loading excitations i.e. as that of seismic forces.

Many finite element softwares are employed nowadays for numerical modeling of structures. They include LS-DYNA, ADINA, CASTEM, PERFORM 3D, SAP, ETABS, ANSYS etc. this study was carried out by using ANSYS software mainly because of the diversity of its input parameters. As the accuracy of a finite element mainly depends upon the proper selection of a numerical model and reasonable finite elements, much time was dedicated to this selection process. The selections of these two components of modeling are based on the degree of computational labor that is needed for processing the results of the finite element model. Research has shown that if homogenous modeling approach is employed with shell and solid elements, it gives reasonable accuracy and suitable computational labor. Heterogeneous modeling does provide more refined results as compared to homogenous modeling but the very high computational labor makes it unfavorable especially for cases where large structures or small structures with refined meshing are to be analyzed.

Due to this and other reasons (mainly convenience and less computation time) it was decided that homogenous modeling technique will be primarily used for the analysis of seismic damage to masonry structures. Heterogeneous models are also formulated for the building units and some of the simpler meshes, in order to compare their results with those obtained from homogeneous

modeling. One other advantage of homogeneous modeling is the ease with which a full scale structure or a structural component can be analyzed with it.

The underlying aim of this comparison is also to gain an in-depth knowledge of the software and to provide an exposure to future researchers at NUST. It will also be used to have an understanding of the input parameters for structural masonry in this software, as ANSYS is not originally coded for evaluation of such geometry. It is evident that 100% accuracy cannot be achieved in numerical modeling to make it in exact agreement with a physical model but a good numerical model is one which reflects maximum features of the actual model. This process of making a model more and more expressive of some actual structures requires refinement of knowledge.

The best way to achieve such a model is to first gather sufficient experimental results of the input parameters so that it can be precisely validated against the results of the numerical model. In this research study, the experimental data from tests performed on masonry prisms and load-deformation results for the masonry units are available to be used for validation of numerical model of them.

4.3 FINITE ELEMENT ANALYSIS OF STONE MASONRY

The data obtained from the ancient stone masonry shear wall test carried out by Vasconcelos (2005) has been used as a base for the present finite element modeling. Prior to the testing of model masonry walls, mechanical tests such as compression, tension and shear tests were done on stone unit, mortar cubes, prisms made out of mortar-less dry-stone, irregular stone with bonding mortar and rubble stone with bonding mortar. These tests on materials were done to determine the elastic, inelastic and strength parameters required for the present finite element modeling. Average compressive strength, tensile strength and Young's modulus of stone was 69.2 N/mm², 2.8 N/mm² and 20200 N/mm² respectively. Average compressive strength of mortar was 3.0 N/mm².

4.4 MESH GENERATION AND ELEMENT SELECTION

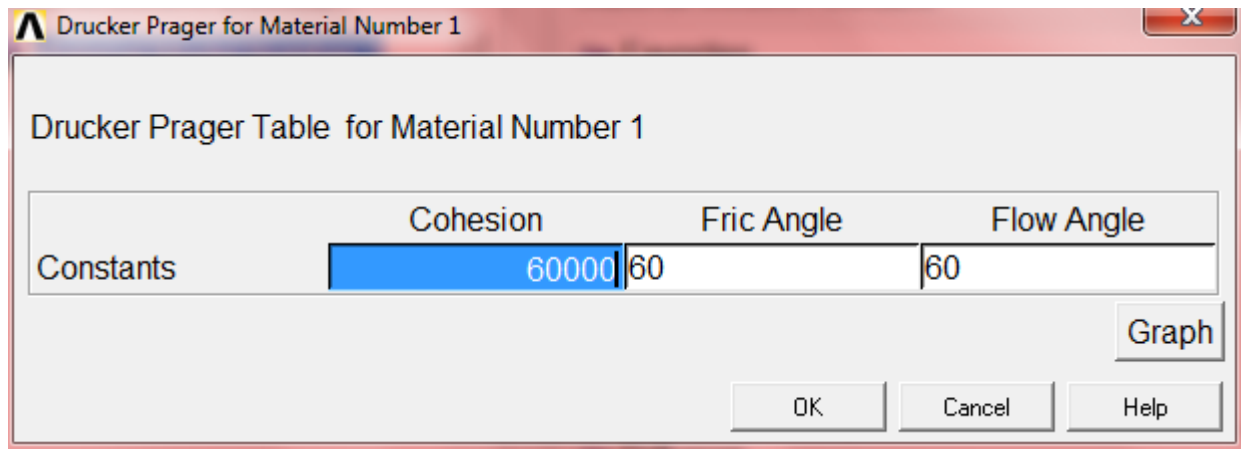
CASE I

For Case 1, following parameters were used as input:

Element Type: SOLID 45

Material Type: Linear Isotropic

Failure Criteria used was Drucker Prager with the inputs as shown below:



The finite element mesh was generated using the software's built-in commands. The following input data was required to generate a mesh for Case I;

- i) whether potential vertical cracks in the middle of the units are to be included in the model,
- ii) whether a masonry joint is to be included in the bottom of the model,
- iii) whether a masonry joint is to be included in the top of the model,
- iv) whether each course contains an integer number of units,
- v) whether the first (bottom) course starts with a full unit or half unit,
- vi) the number of masonry courses in the model,
- vii) the number of complete units per course,
- viii) the number of divisions (finite elements) per unit in the x direction,

ix) the number of divisions (finite elements) per unit in the y direction,

x) the width of the units (plus $\frac{1}{2}$ of thickness of the mortar joint),

xi) the height of the units (plus $\frac{1}{2}$ of thickness of the mortar joint),

xii) the half of a thin fake joint thickness for joints, only for visual or identification purposes.

The below figure shows division of units in x and y directions, interface around the unit and fake thickness of joints.

As the experimental test results showed no cracks in the unit, potential cracks in the units were not considered in the entire modeling work for Case 1.

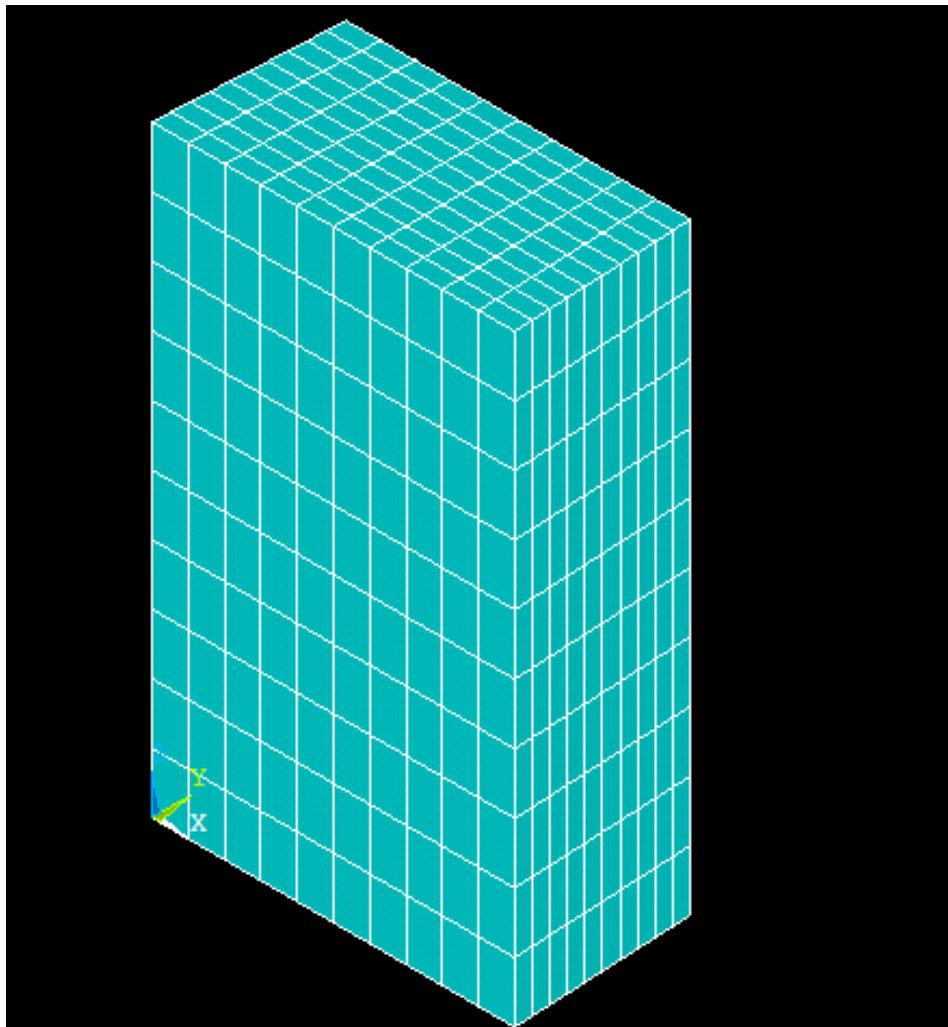


Figure 4.1. Element plot of FE model

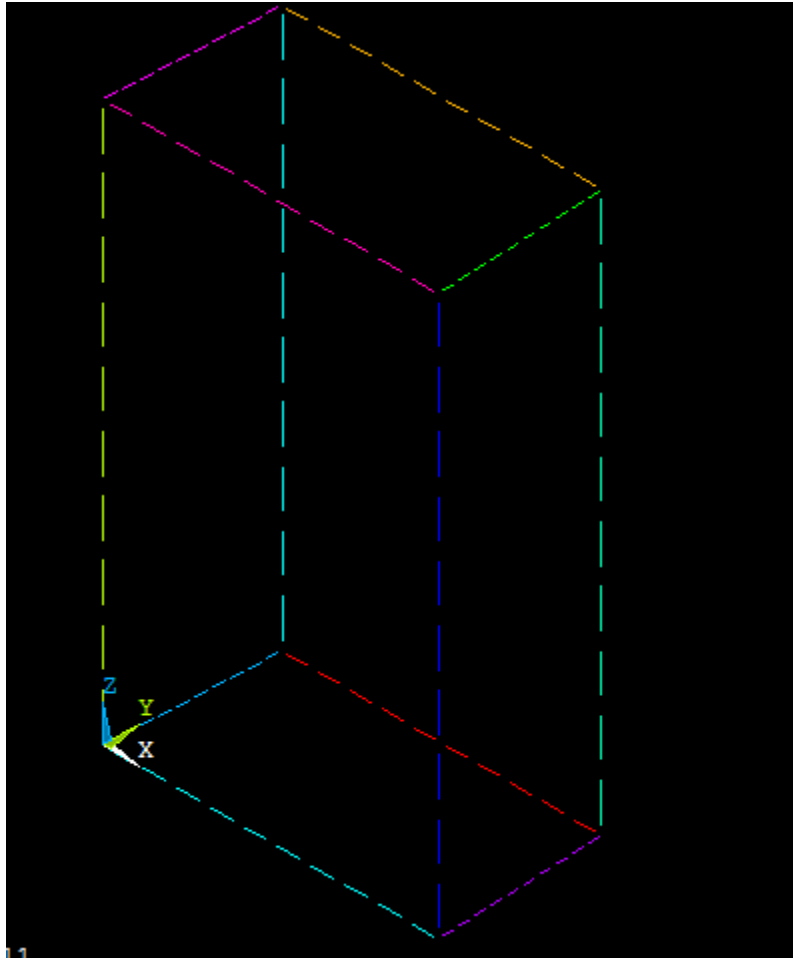


Figure 4.2. Lines plot of FE Model

4.5 MATERIAL PROPERTIES (STRENGTH, ELASTIC AND INELASTIC PARAMETERS)

The average Young's modulus of dry-stone prisms was 14800 N/mm² (based on test results of four prisms built with four course dry-stacked stones). Young's modulus of large walls is usually different from the Young's modulus measured in small test specimens. This phenomenon has been found and reported by Lourenço (1996a). Micro modeling approach based on interface finite elements requires two distinct stiffnesses, namely, the stiffness of the stone units and the stiffness of the joints. Once the stiffness of the stone units is known, the stiffness of the joints can be calculated from the experimental axial pre-compression load-displacement curve of the walls.

Normal joint stiffness (K_n, joint) was calculated using the following formulation proposed by Lourenço (1996a) in which the wall is considered as a series of two springs in vertical direction, one representing the stone and the other representing the joint.

$$K_n, \text{joint} = 1/(h(1/E_{\text{wall}} - 1/E_{\text{stone}})) \text{-----} (1)$$

where

K_n, joint = Normal joint stiffness

h = Height of stone (150 mm)

E_{wall} = Young's modulus of wall

E_{stone} = Young's modulus of stone

The tangential stiffness (K_s, joint) was calculated directly from the normal stiffness using the theory of elasticity as follows, Lourenço (1996a):

$$K_s, \text{joint} = K_n, \text{joint} / 2(1 + \nu) (2)$$

where

K_s, joint = Normal joint stiffness

ν = Poisson's ratio (0.2)

The following inelastic properties of unit-mortar interface were taken into account (Lourenço & Rots [1997]):

i) Tensile criterion: f_t (tensile strength) and G_I

f (fracture energy for Mode-I);

ii) friction criterion: c (cohesion), $\tan \phi$ (tangent of the friction angle),

$\tan \psi$ (tangent of the dilatancy angle) and Mode-II fracture energy, G_{II} ;

iii) cap criterion: f_c (compressive strength) and G_{cf} (compressive fracture energy).

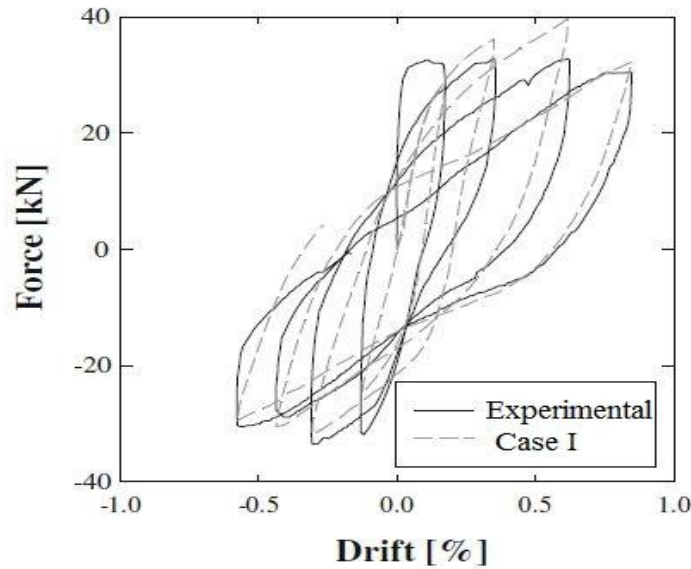
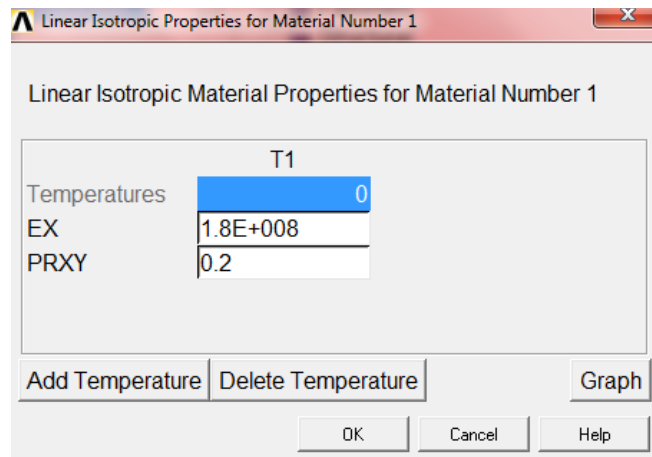
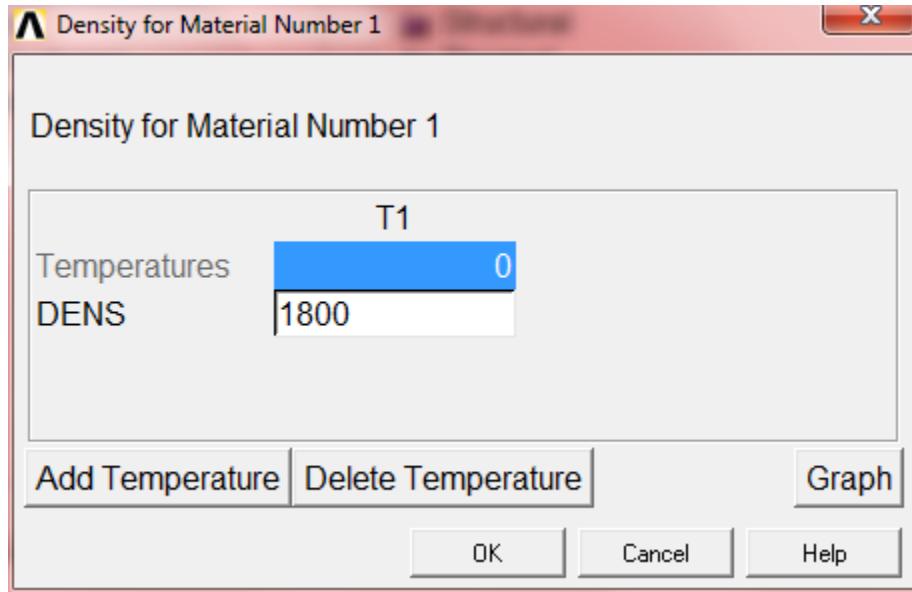


Figure 4.3. Force vs Drift for Case I

The inelastic parameters required for the analysis were extracted from Vasconcelos (2005), when available, or followed the recommendations given in Lourenço (1996a). Again, note that the elastic stiffness of the interfaces was adjusted from the measured experimental results, becoming clear that the stiffness decreases consistently from Case I to Case III, due to the increasing thickness of the joint and irregular shape of the units. The equations that govern the inelastic behavior of masonry are given in detail in Lourenço and Rots (1997), where it is assumed exponential softening for tension and for shear, followed by parabolic hardening, parabolic softening and exponential softening in compression.

Following are details of material model used in Case 1:





4. 6 GEOMETRY DEFINITION

The geometry of the pier was outlined through the creation and extrusion of a base area defined by 4 key points.

k,1,0,0,0

k,2,1.57,0,0

k,3,1.53,0.80,0

k,4,0.04,0.80,0

l,1,2,

l,2,3,

l,3,4,

l,4,1,

AL,1,2,3,4

VOFFST, 1, 2.61,

Defined the geometry, n hard point were created. These hard points mark the position of the displacement transducers used in the experimental test.

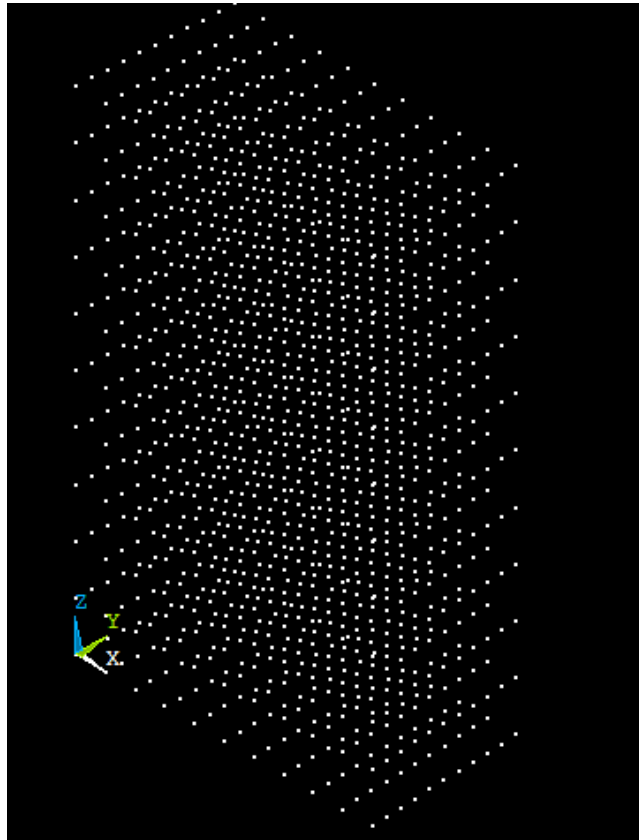


Figure 4.4. Nodes for the FE model

4.7 DEFINITION OF THE LINEAR PROPERTIES OF THE MATERIAL

The linear properties of the masonry were defined based on a previous numerical model calibrated for a masonry pier with similar material characteristics. The values assumed are those as shown in above figures. The masonry pier has been modeled by mean of SOLID95 elements. SOLID95 is a higher order version of the 3-D 8-node solid element SOLID45. The main advantage of this element is that it can tolerate irregular shapes without as much loss of accuracy.

Following is the command line for input of entire material model data for Case 1:

```
ET,1, SOLID95
```

MPTEMP, , , , , , ,

MPTEMP, 1, 0

MPDATA, EX, 1, 1.80E08

MPDATA, PRXY, 1, 0.20

MPDATA, DENS, 1, 1890

Meshing:

The geometry was converted into a finite element mesh, composed of 3D solid irregular elements, (SOLID95) to represent the masonry. The size of the finite elements was defined by the division into segments with 0.15 m length.

VSEL, , , , 1

VATT, 1, , 1, 0

LESIZE, ALL, 0.15, , , , , ,

MSHKEY, 0

MSHAPE, 1, 3d

VMESH, 1, 2

Application of Loads and Displacement Constraints

The model is displacement constrained at the base in the X, Y and Z directions.

DA, 1, UX, , 0

DA, 1, UY, , 0

DA, 1, UZ, , 0

The standard Earth gravity acceleration was applied in n sub steps (1st load step) and the outputs in terms of results defined.

```
ANTYPE,0
```

```
TIME,0
```

```
NSUBST,15,15,15
```

A time-variable displacement used to simulate the experimental imposed displacement was applied at the hard point created to the effect. Finally, the 2nd load step was defined in n sub steps and the outputs selected.

```
*DIM,DISP,TABLE,501,1,0,TIME,Y, ,0
```

```
*TREAD, DISP, C:\Numerical_Models\Disp_17_MONO_10, txt, , 0
```

```
DK, 9, , %DISP% , ,0,UY, , , , ,
```

```
OUTRES, ALL, ALL
```

```
LSWRITE,2,
```

```
Time, 501
```

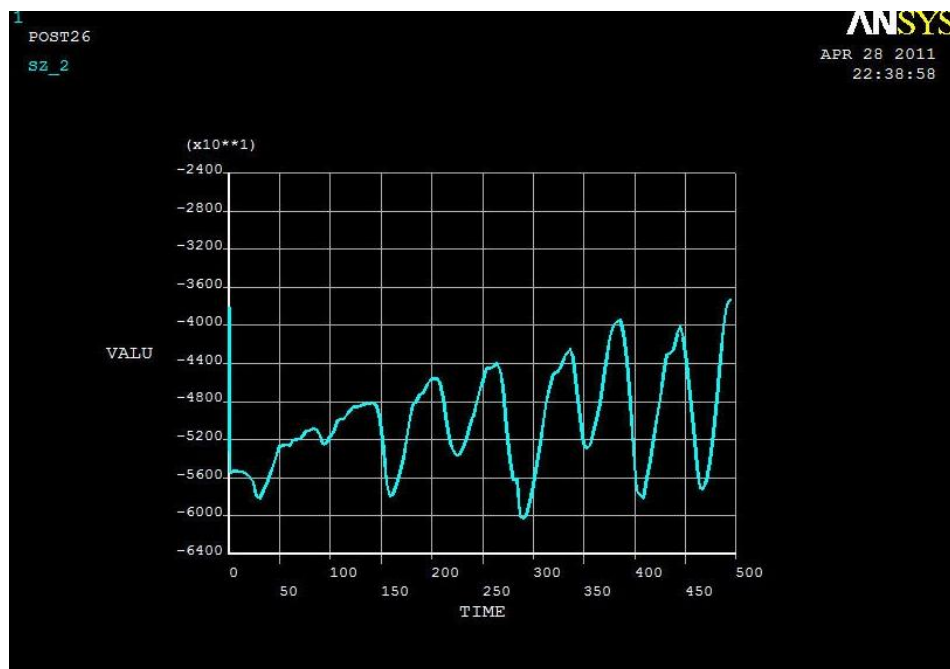


Figure 4.5. Cyclic application of vertical load only

4.8 NUMERICAL ANALYSIS

Static and dynamic analysis has been carried out on a 3D model of the stone masonry pier using the FE computer code ANSYSr V12.0.

The masonry have been modeled using SOLID95 elements, which exhibits quadratic displacement behavior and were defined by 20 nodes each with 3 degrees of freedom. The 3D model is composed by X nodes and X elements.

The physical properties of masonry material have been established based on static analysis described in the literature.

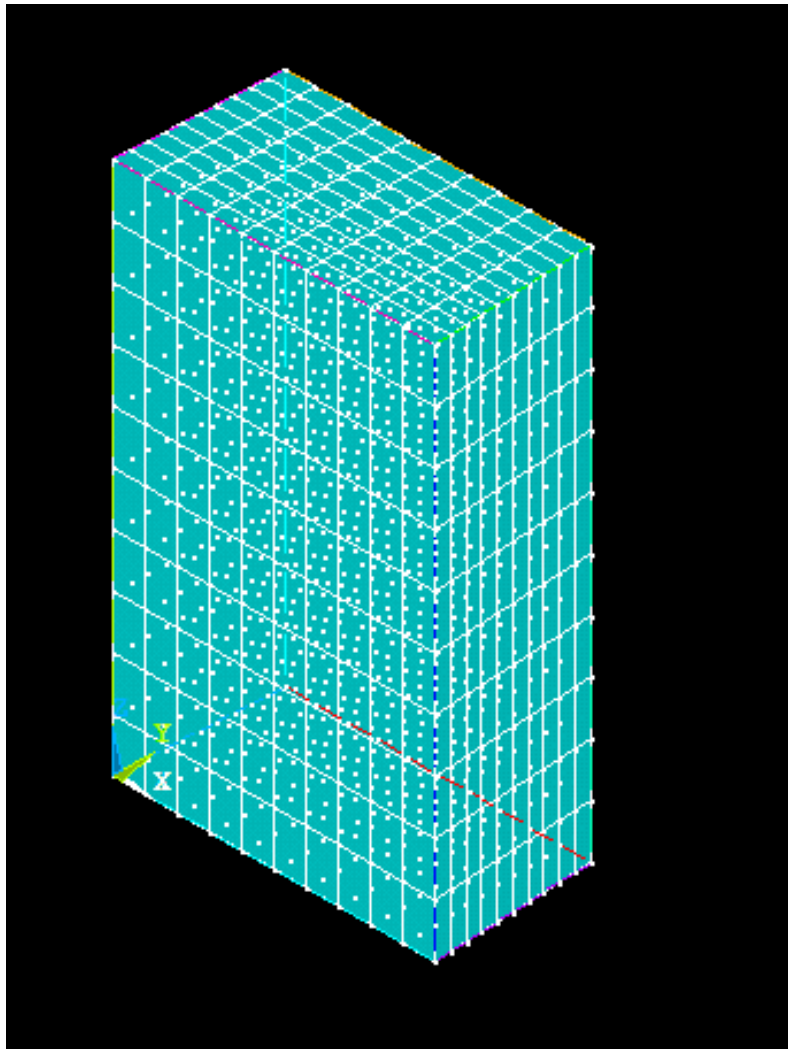


Figure 4.6. Multi Plot of the FE model

4.9 LINEAR STATIC ANALYSIS

After the model calibration a linear static analysis was carried out. The stress resultant distribution and the vibration mode shapes obtained with the numerical model were studied for Case 1.

Firstly (step-1), the desired total vertical pre-compression load (either 100 kN or 175 kN or 250 kN) was divided into small steps and gradually applied on the top surface of stiff steel beam. Then the horizontal load in terms of incremental displacement was applied in small steps at the top right corner of the steel beam (step-2).

For a good insight into the stress distribution at different horizontal load increments, the horizontal displacement was increased gradually to 2.5 mm, then to 5 mm, then to 10 mm and lastly until the failure/ collapse, which provided the behavior of each critical region of the walls, in addition to the overall deformation characteristics.

The vertical and horizontal loads were applied in small steps to achieve a converged solution, particularly in the case of dry stone masonry, which features no tensile strength or cohesion.

4.10 FEM ANALYSIS RESULTS

Results of the nonlinear finite element analysis were post processed and are presented in this section. Axial pre-compression load, lateral shear load and material properties are the main parameters that significantly influenced the behavior of the shear walls. Load flow in the whole body of the wall at different lateral displacement levels, failure modes and state of load and displacement in critical nodes are presented in the following figures.

These FEM results are compared with the actual model through relations between various parameters such as:

- Drift vs Force diagrams
- Crack propagation in actual and numerical model
- Stress vs Strain plots for actual specimen and different cases of the numerical model
- Stress concentration in various FE models

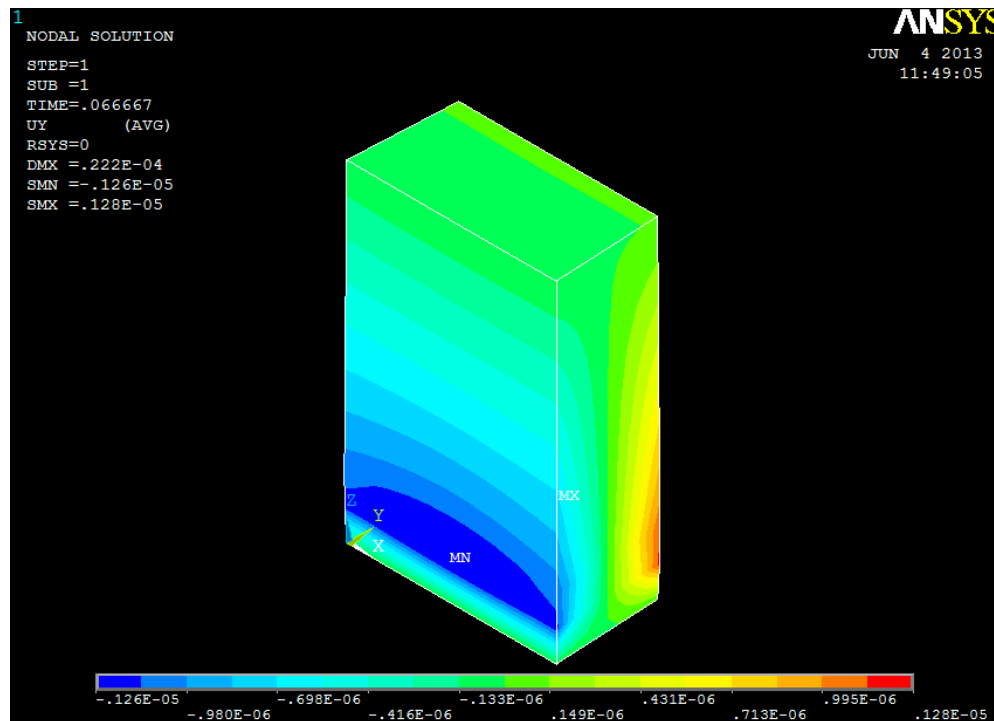


Figure 4.7. Contour plot for XY principal shear

4.11 MODES OF FAILURE

Heel, toe, centre and local point of application of load on the shear wall are the critical regions. Failure in these regions mainly controlled the overall behavior of the shear walls. Walls failed due to either flexure or racking or toe crushing or tensile cracking at the heel followed by shear failure along the diagonal. Combination of two or more failures has also occurred at critical load level. At lower pre-compression levels (100 kN), walls usually failed due to a progressive flexural mechanism characterized by heel cracking followed by rocking and toe crushing. Irrespective of masonry types, axial pre-compression stress significantly influenced the behavior of the shear walls. A small increase in vertical load provided the walls with a larger strength due to the improvement of bond resistance mechanisms between joint and masonry units. A substantial increase of axial stress changes the failure mode of the wall from flexure to shear.

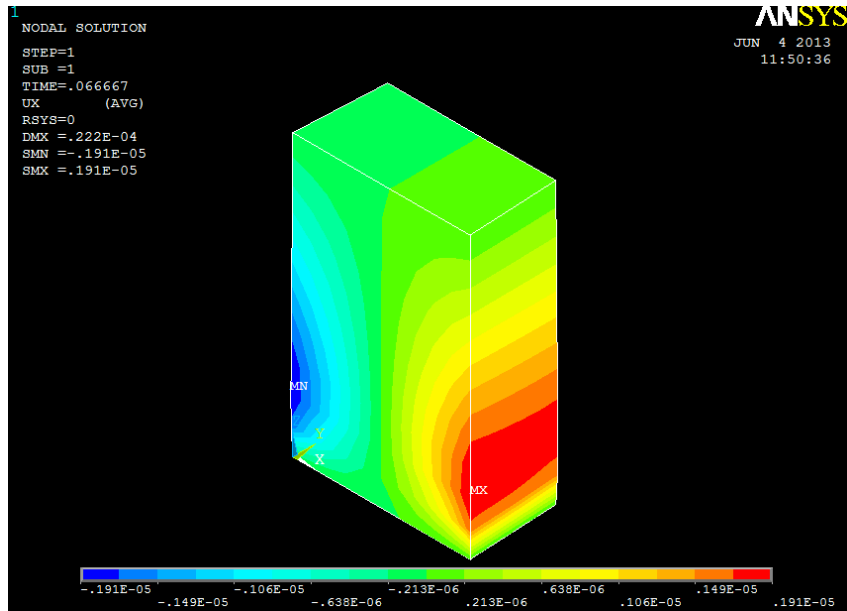


Figure 4.8. Contour Plot for ZY principal shear

Lower axial pre-compression load caused flexural or rocking failures and higher pre-compression load caused rocking, toe crushing, crushing at region of load application and diagonal shear failures along the diagonal direction. Flexural cracking in the bed joints occurs when the tensile stress on a horizontal mortar joint exceeds the sum of the bond strength of that mortar joint and the frictional stress between the mortar and the units.

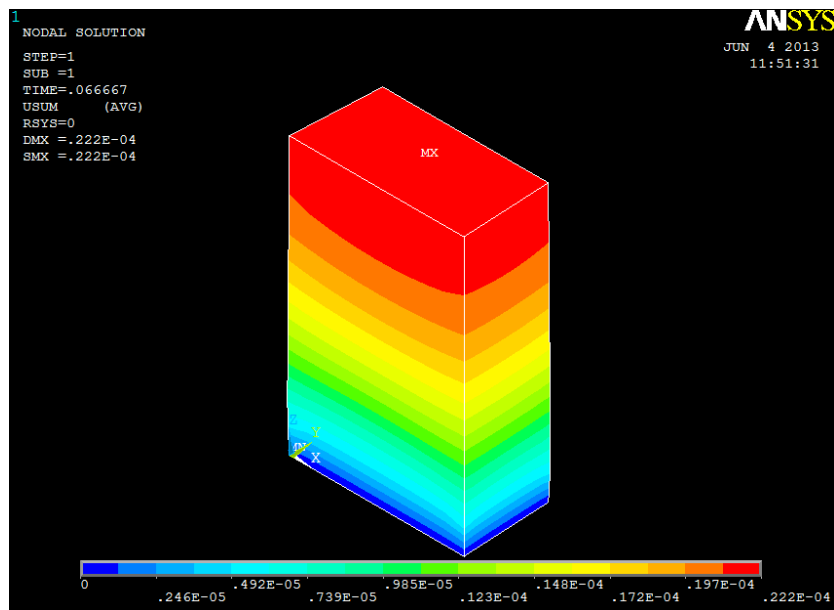


Figure 4.9. Contour Plot of model when subjected to uniaxial monotonic loads only

Rocking mode of failure occurs due to overturning caused by either low level of axial load and/or weak tensile bond strength of mortar joints dominated. Diagonal shear failure occurs when the diagonal tensile stress resulting from the compression shear state exceeds the splitting tensile strength of masonry. The following figure details the progress of cracking and redistribution of compressive stresses upon loading, which leads to a series of struts defined by the geometry and stone arrangement.

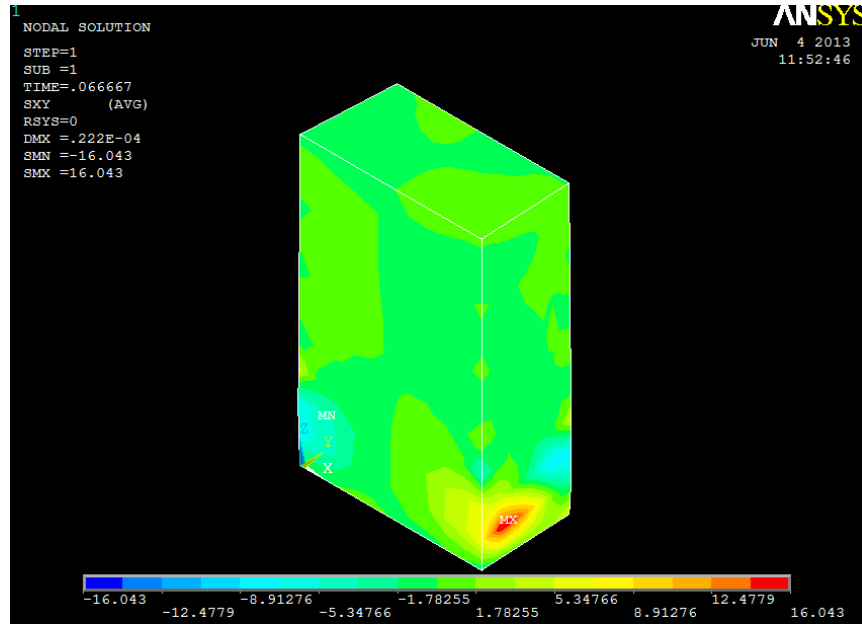


Figure 4.10. Contour plot for ZX principal shear

For a good insight into the stress distribution at different horizontal load increment, the horizontal displacement was increased gradually to 2.5 mm, then to 5 mm, then to 10 mm and until the failure/ collapse, which provided the behavior of the critical regions at different magnitude of applied loads. When the applied displacement is 2.5 mm, a larger number of diagonal compressive struts are clearly formed and the whole wall is still mostly structurally sound. As the displacement increased from 2.5 mm to 5 mm and then to 10 mm etc, the number of compression struts reduced and diagonal cracking started to occur. A complete diagonal crack propagates and the failure mode is mostly controlled by shear, together with localized rocking of the cracked stone pieces in the compressed toe region of the wall. The large number and variability of the material parameters necessary to characterize the developed model permits to adopt a set of parameters suitable to closely fit the experimental capacity slenderness ratio

diagrams. This agrees reasonably well with the failure mechanisms observed in experimental tests.

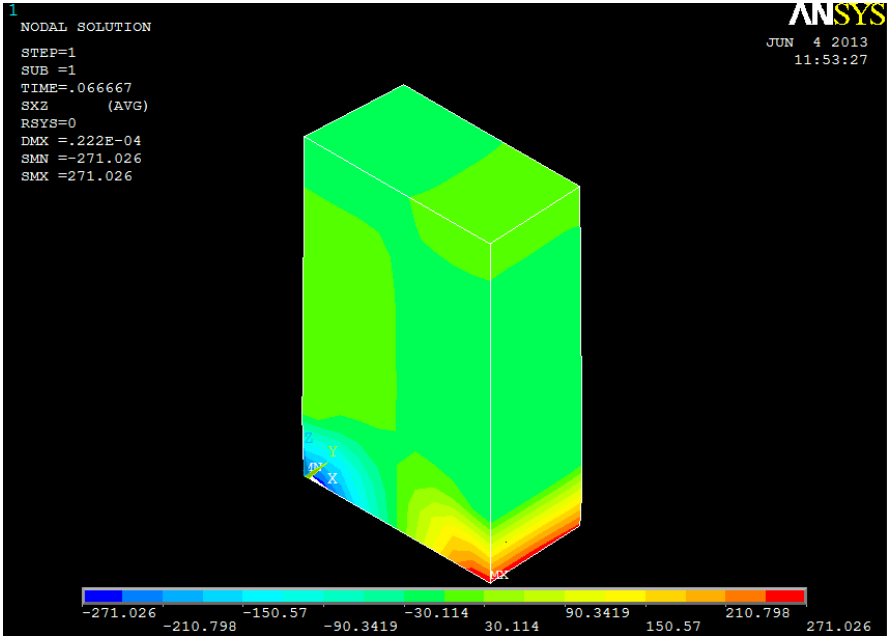


Figure 4.11. Contour plot for principle shear in Y direction



Figure 4.12. Cracking Pattern in actual specimen

The failure of Case II, irregular masonry is not so different from Case I, even if the orientation of the diagonal crack is different and more shear failure is apparent. The deformed shape of original mesh of Case III will be discussed in subsequent sections. Unexpectedly, the model failed in sliding along a weak plane at about mid-height, at very low level applied lateral load. This clearly indicates that failure is influenced by the irregular internal arrangement and unrealistic results can be obtained.

From the contour plots for shear in Y plane, it can be observed that the initial crack starts at the toe in compression. This is very much in agreement with the actual test results as shown above.

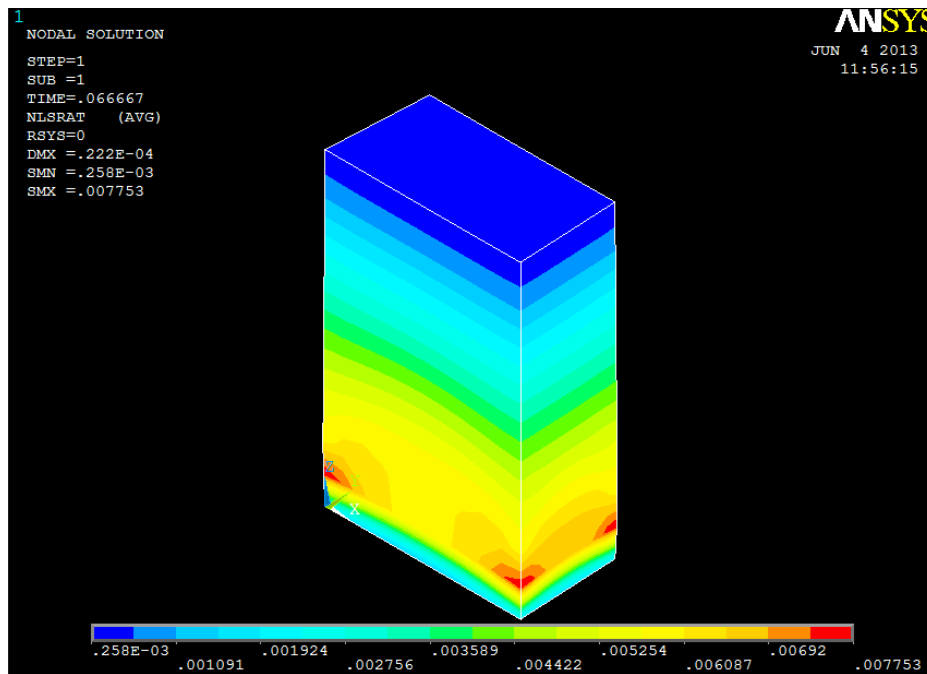


Figure 4.13. Contour plot for elastic strain in X axis

To avoid the sliding failure, a shear key along the weak plane was provided by adding an extra corner to a four corner stone unit at middle of the weak plane/ path, and the original mesh was modified. The modified mesh was subsequently used in all analyses. Moreover, as the internal structure is not symmetric, the results are provided from Left to Right loading (L-R) and Right to Left loading (R-L). The deformed shapes at collapse for the modified mesh are. Under different pre-compression levels, the failure occurred in the modified Type III mesh is not so different

from the Type I and II masonry particularly at higher level of axial pre-compression load, including a diagonal shear crack and toe crushing. Certainly that a major difference is that not really stepped cracks are found, being the crack mostly straight.

4.12 LOAD-DISPLACEMENT CURVES

From the experimental cyclic hysteresis curves, the peak load points were used to establish experimental load-displacement envelope curves. These experimental curves are compared with numerical results, and presented in figures below for Type I, II and III masonry respectively. As mentioned in section 2, monotonic tests were performed for Type I (regular/ sawn) masonry only.

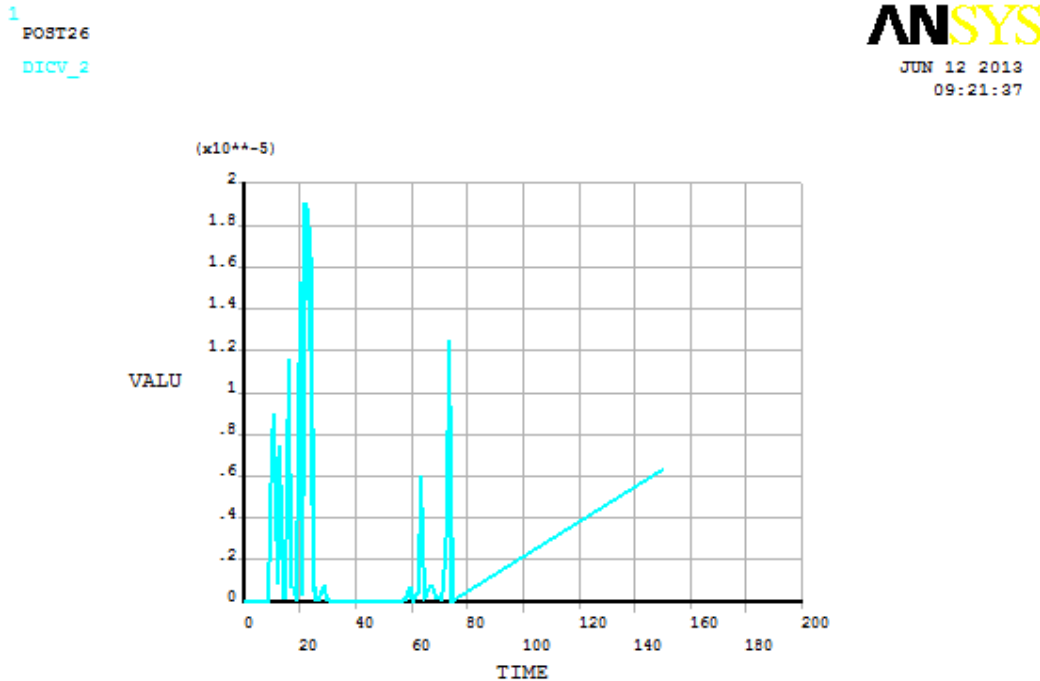


Figure 4.14. Displacement of top surface of FE model when subjected to first cycle of loading

The load-displacement envelope curve obtained under monotonic loading was superimposed with the envelope curves of cyclic loading and presented below. As can be seen from the figure, these two (monotonic and cyclic) curves follow exactly a same path until the appearance of first crack at about 60-80% of failure load. After the appearance of crack in ascending zone, these two

curves still follow the same path with little difference that can be neglected. After reaching close to failure, these two curves stabilize and follow exactly the same path again with increasing displacement and almost constant load level. Similar finding has been reported by Senthivel and Sinha (2002) for masonry subjected to monotonic and cyclic loading. For the rest of the case (II and III), it was assumed that the peak points of cyclic hysteresis curves approximately coincides the monotonic envelope curve.

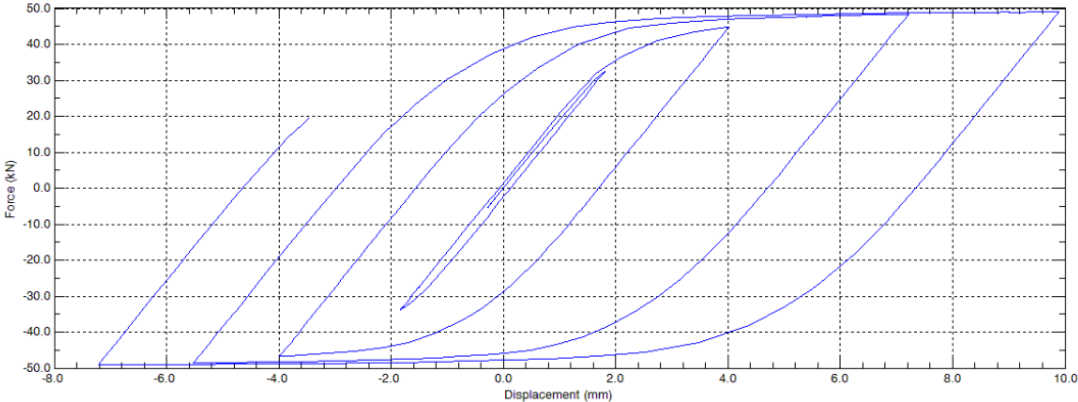


Figure 4.15. Force-Displacement Curve for Case I

Envelope curves of Case I masonry exhibited three different rages and trends: an initial linear portion with a high rate stiffness (which is directly proportional to the applied axial pre-compression load) followed by a transitory non-linear portion and, finally a relatively approximate linear portion with slow rate of increase in load and faster rate of increase in displacement.

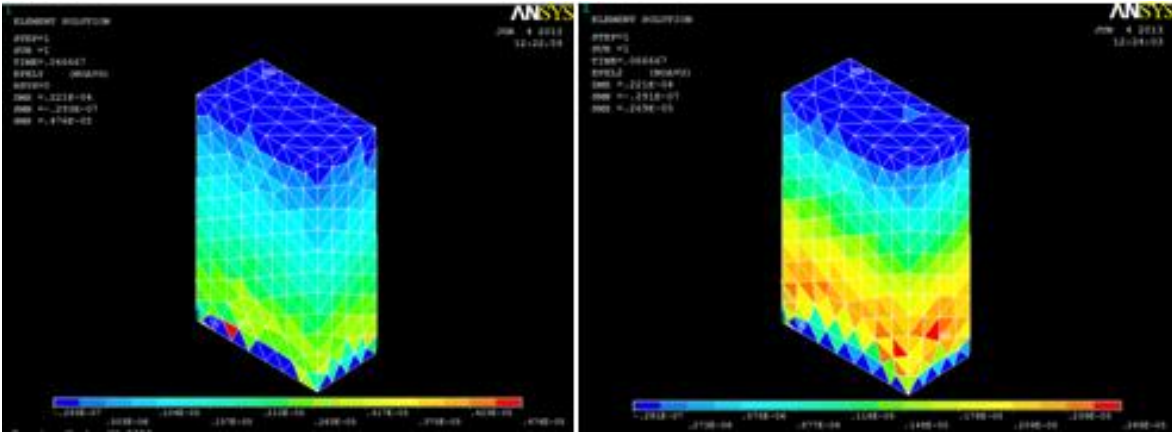


Figure 4.16 (a) Elemental Plot of crack, showing initial cracks in toe of the pier

The similar trends can be seen in the case of Case II and III masonry except for the sudden load drops occurred in the ascending branch of the curves due to movements or sliding of stones. Initially, the curves exhibited large stiffness with linear behavior up to about 30% of the respective peak load. As the lateral load increases, stiffness degradation takes place. A good correspondence between numerical and experimental load-displacement curves has been found for Case I and Type II masonry.

In case of Case III, due to irregular and random assembly of units with different size and texture, the load-displacement response was sensitive to the direction of lateral load.

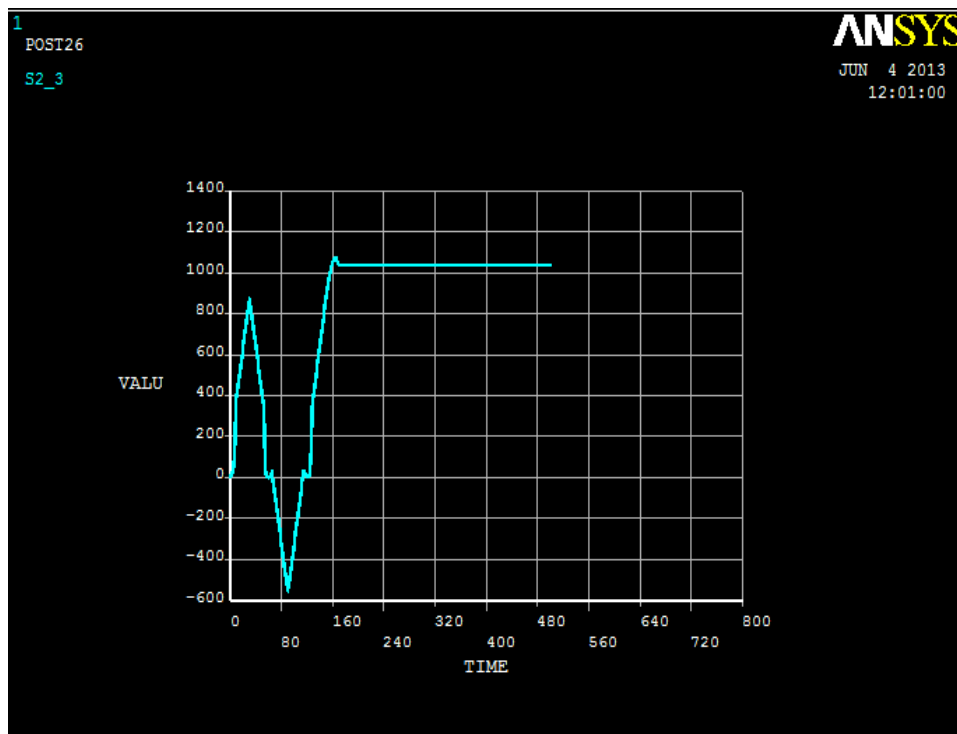


Figure 4.16 (b) Elastic strain during 1st cycle of loading

This leads to a significant scatter of the results and less good agreement in the results, particularly for the case of higher pre-compression. Still, the asymmetry of the results can be replicated by the numerical results. Possibly, better agreement could be obtained by fine tuning the adopted shape of the units for each test, but this is outside the scope of this thesis work.

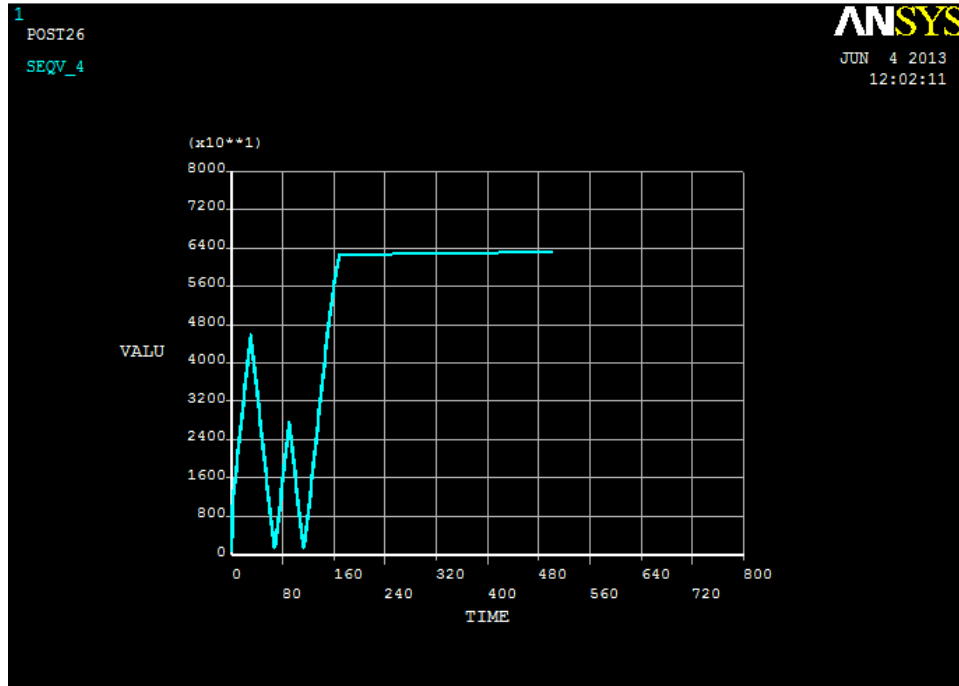


Figure 4.17 Elastic strain during 2nd cycle of loading

Finally, it is noted that the model of Lourenço and Rots (1997) is not capable of reproducing adequately the crack closure and cannot be used for reversed cyclic loading.

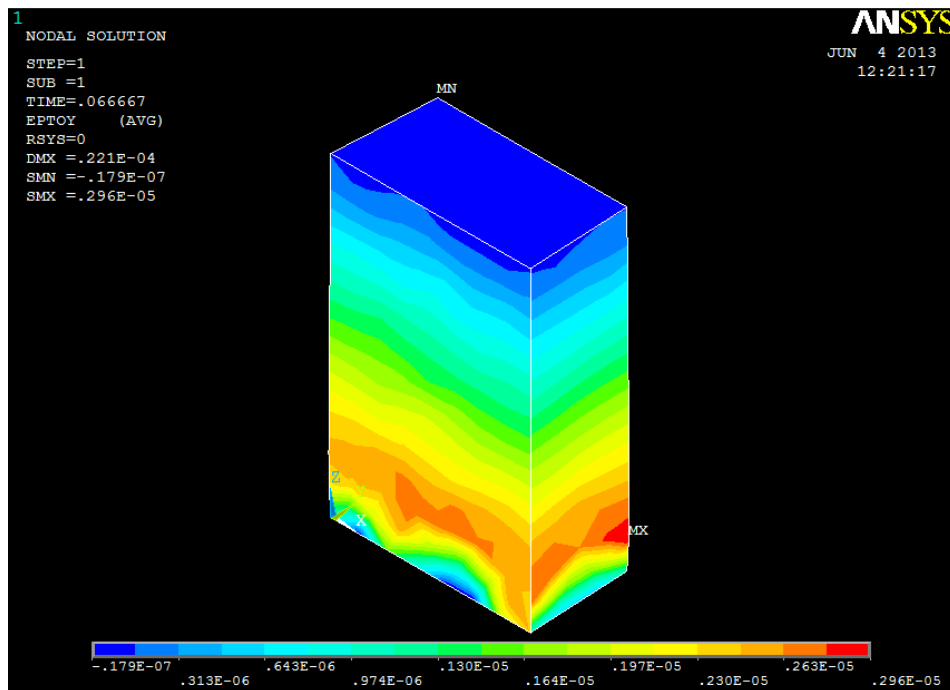


Figure 4.18 Propagation of cracks

The cyclic loading model available, Oliveira and Lourenço (2004), requires significant additional data and experiences severe convergence difficulties upon a large number of cycles or large displacements, being the monotonic model much more robust.

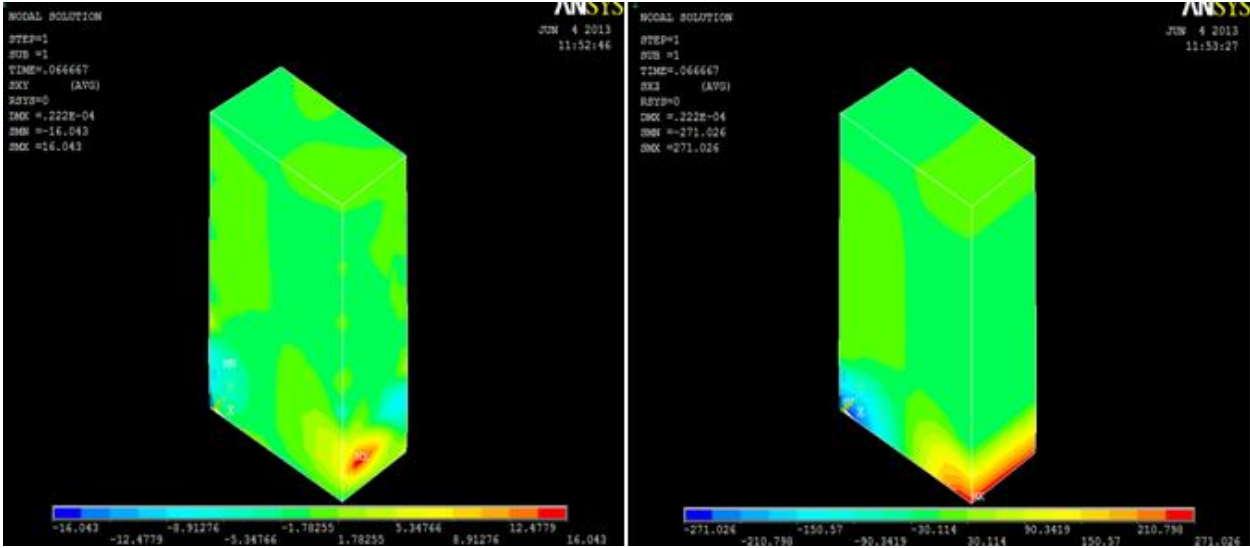


Figure 4.19 Principle Stress Concentration at toe of Wall

The combination of dry stacked masonry, which requires very small steps due to lack of tensile strength and cohesion, with cyclic loading makes the analysis process unwieldy. Therefore, no attempt is made here to replicate the cyclic results of the experimental testing program. It seems that more robust material models are needed for this purpose.



Figure 4.20 Cracking pattern in Actual specimen

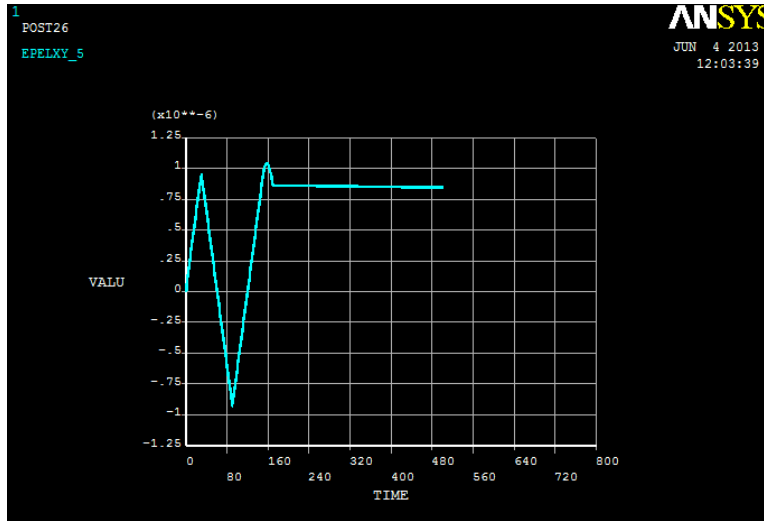


Figure 4.21 Stress intensity for 1st cycle of loading

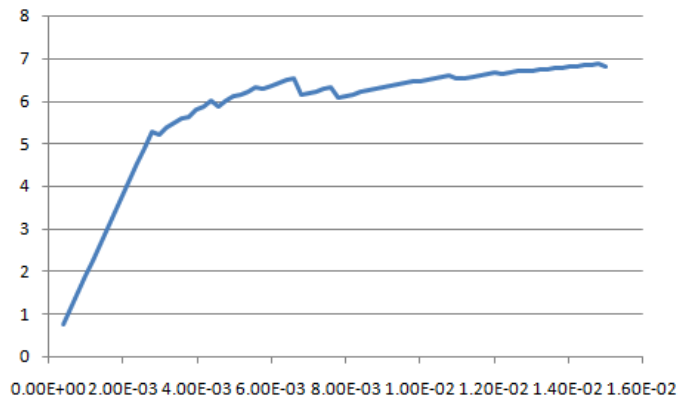


Figure 4.22 Stress-Strain Plot of the entire model for Case I

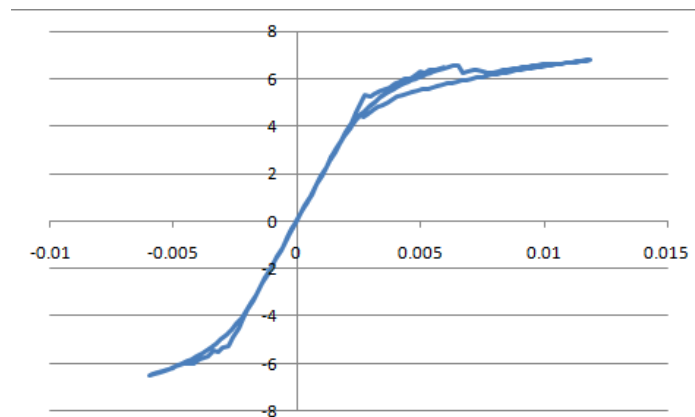


Figure 4.23 Displacement with respect to Time for entire loading of the model in Case I

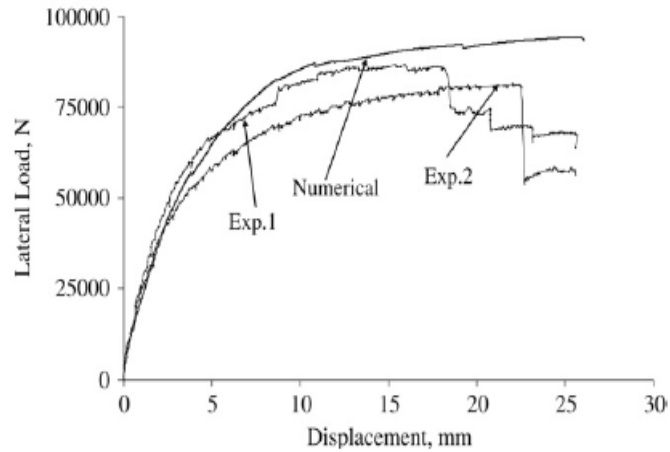


Figure 4.24 Comparison of numerical and experimental results for Case I

4.13 VARIATION IN MATERIAL PROPERTIES' PARAMETERS

CASE II

- In Case II instead of simple Drucker Prager, modified Drucker Prager model, was used.
- Additional properties for masonry when material is assumed to be non-linear inelastic
 - $f_{cDP} = 757$ Pa (uniaxial compressive strength)
 - $f_{tDP} = 223$ Pa (uniaxial tensile strength)

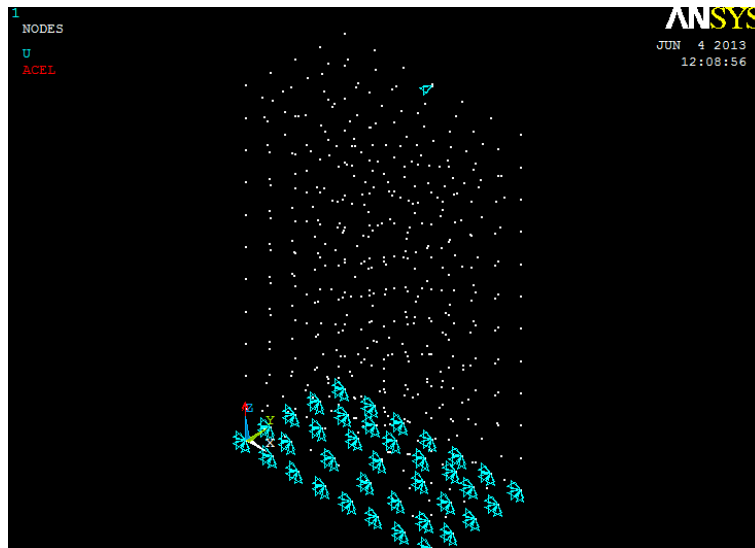


Figure 4.25 Nodal plot for Case II

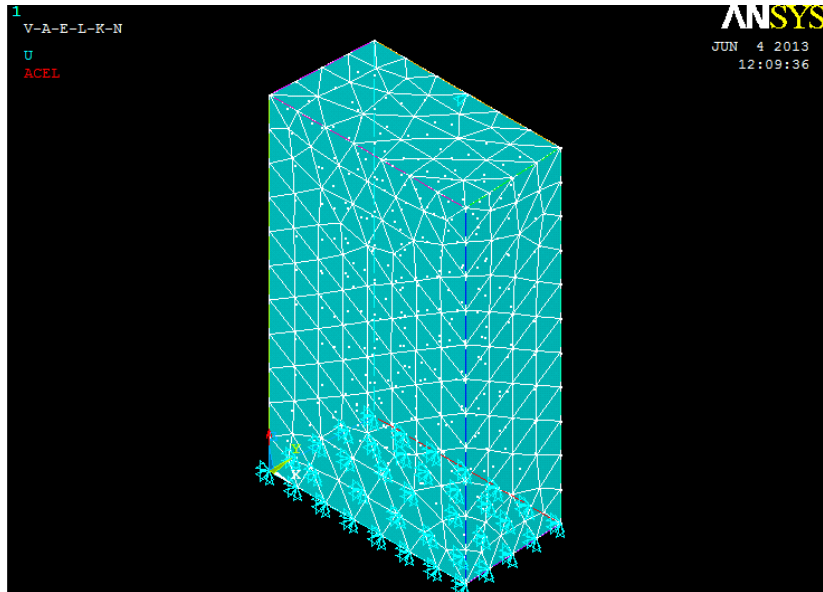


Figure 4.26 Elemental plot for Case II

For Case 2 following parameters were used as failure criteria:

DP yield criterion:

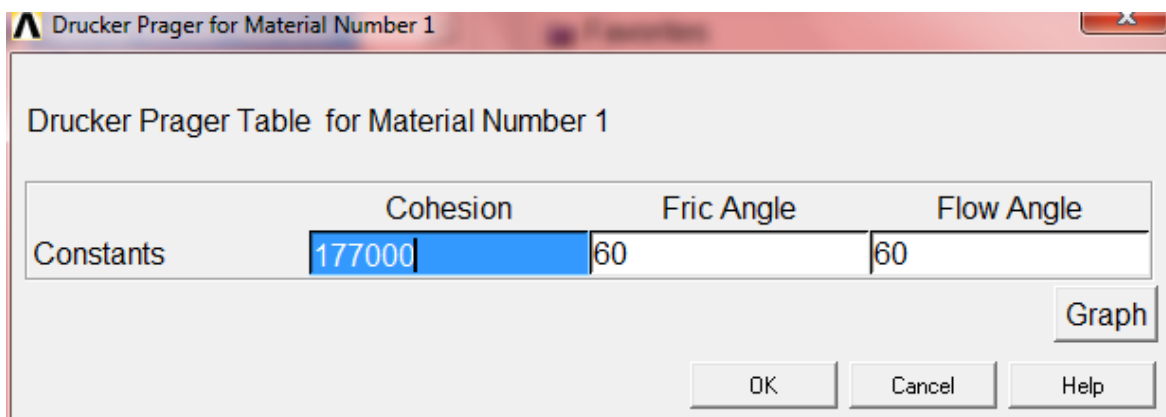
c (cohesion): 0.177 MPa

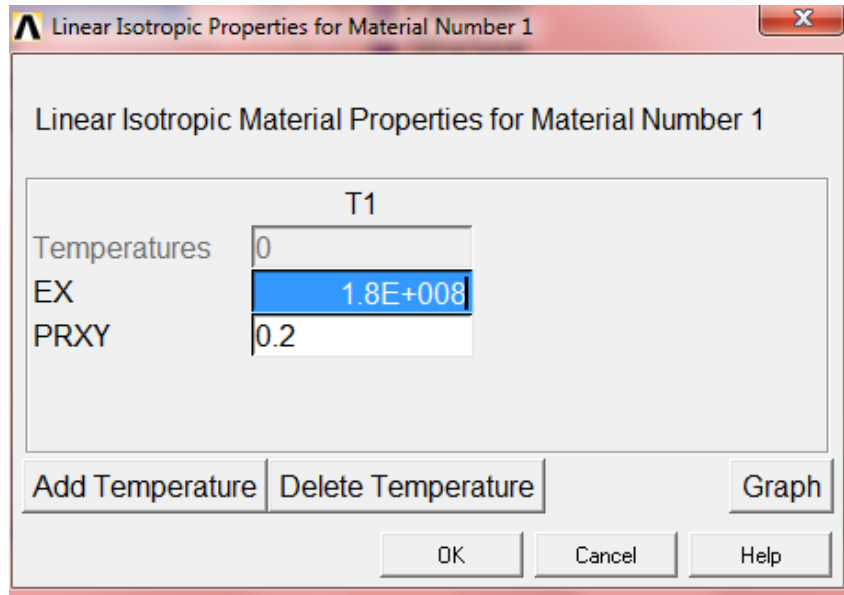
η (flow angle): 40°

ϕ (friction angle): 40°

f_{cDP} (uniaxial compressive strength): 0.757 MPa

f_{tDP} (uniaxial tensile strength): 0.223 MPa





In the numerical simulation for Case II, the units were modeled by using plain-stress continuum 8-node elements and for the mortar joints adopted 6-node zero-thickness line interface elements. In addition, hinges are modeled by means of stiff triangular objects.

1
POST26
DICV_9

ANSYS
JUN 12 2013
10:05:32

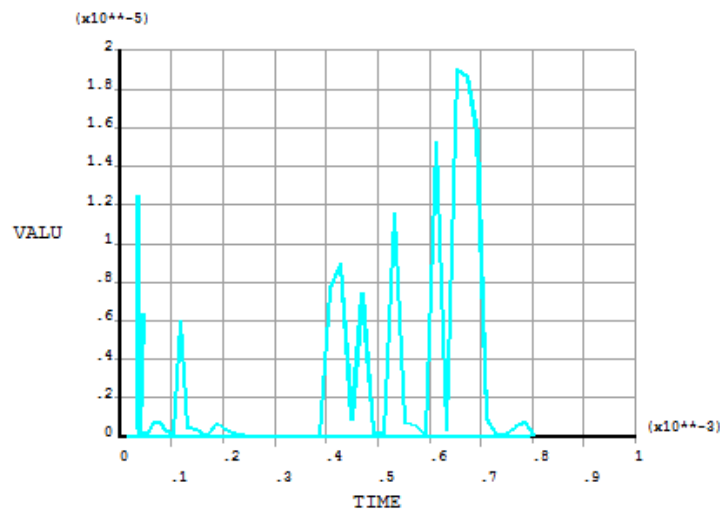


Figure 4.27 Displacement for top surface of pier for Case II

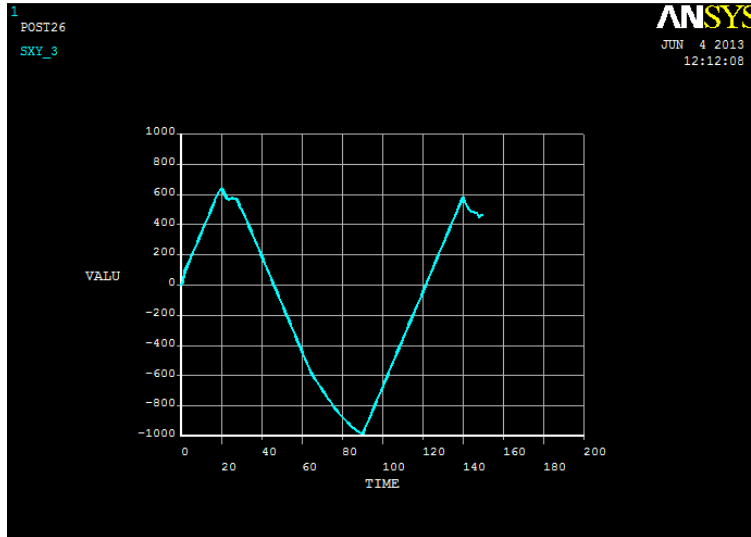


Figure 4.28 Elastic Strain plot for 2nd cycle of loading for Case II

Each unit was modeled with 12 x 3 elements. Some parameters have been taken directly from the previous research. The fracture energy for model have been taken from the test carried out by Van der Pluijm (1992) and for the parameter of shape of elliptical cap b_7 a value of 9 has been adopted from Lourenco (1996).

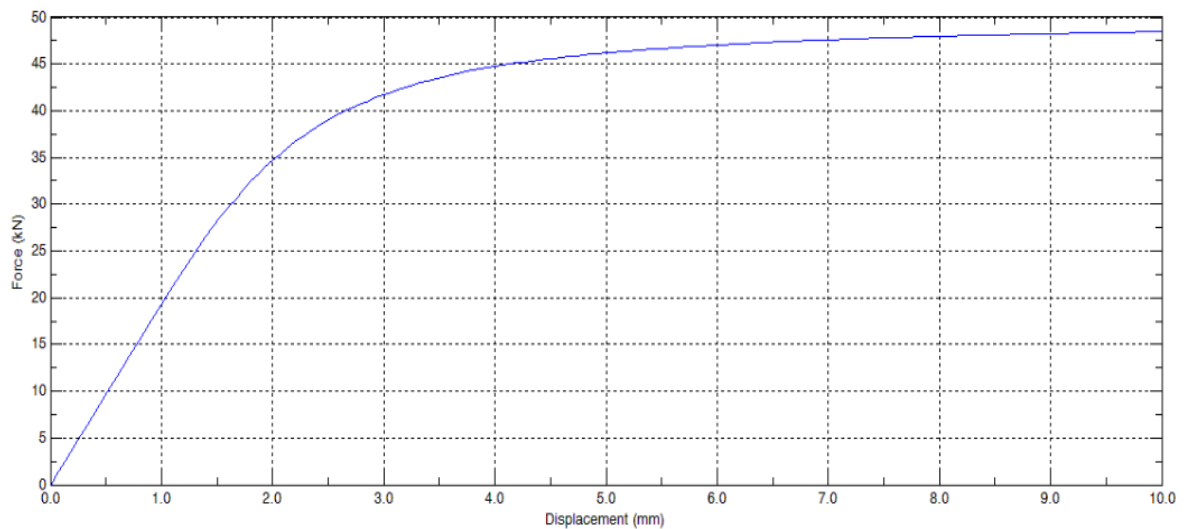


Figure 4.29 Force displacement curve for Case II

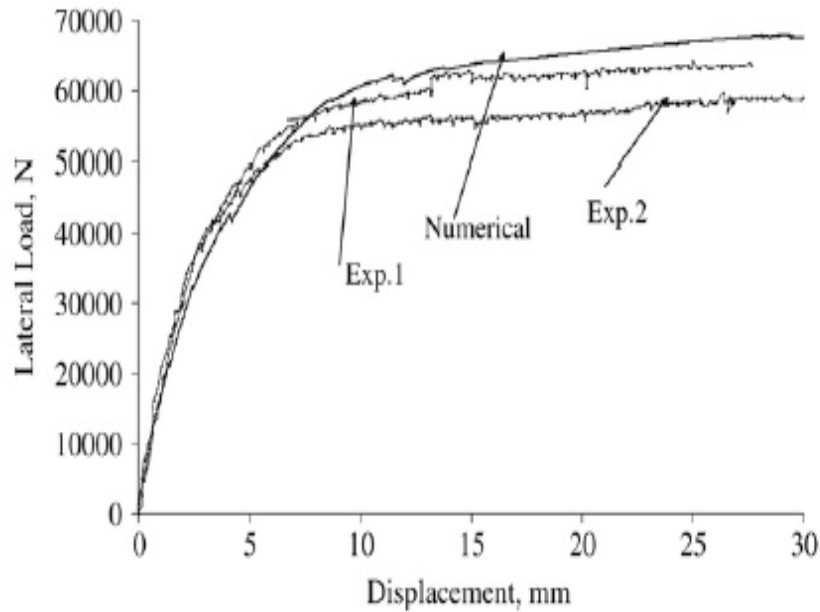


Figure 4.30 Comparison of numerical and experimental results for Case II

The interface elastic stiffness values were calculated from thickness of the joint the Young's moduli of unit and joint respectively, and the shear moduli of unit and joint, respectively as CUR (1994). The different strength values have been obtained from the experimental study carried out in UPC (2009). The compressive fracture energy and equivalent relative displacement, calculated according to Model Code 90 and Eurocode 6, respectively by using formula given by Lourenco, (1996).

4.14 BOUNDARY CONDITION AND LOADING

For all cases, micro-models of wall considered hinged-hinged configuration. The hinges are modeled by means of stiff triangular objects placed at the bottom and at top of the wall, whose end vertex is allowed to freely rotate. The vertical load was applied concentrically and eccentrically as unit deformation. The boundary condition and loading configuration is shown in the following figures.

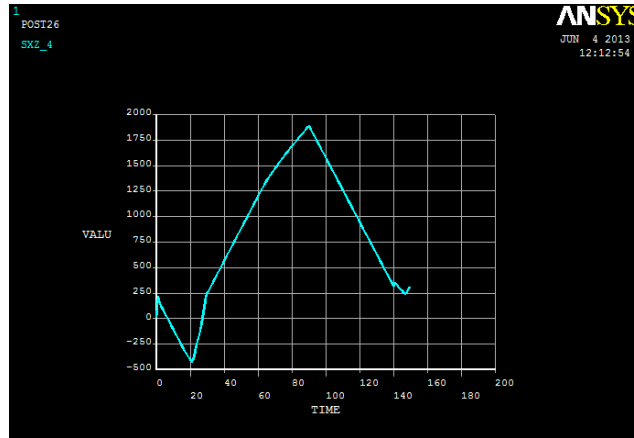


Figure 4.31 1st principal stress for 1st cycle for Case II

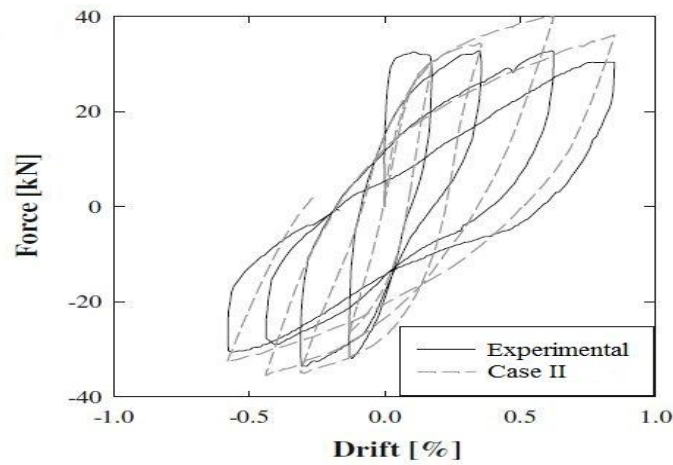


Figure 4.32 Storey Drift vs Force diagram for Case II

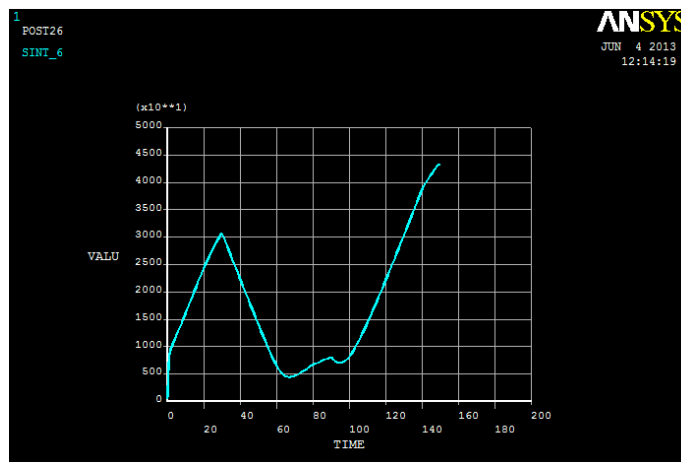


Figure 4.33 XY shear stain plot for 3rd cycle of loading for Case II

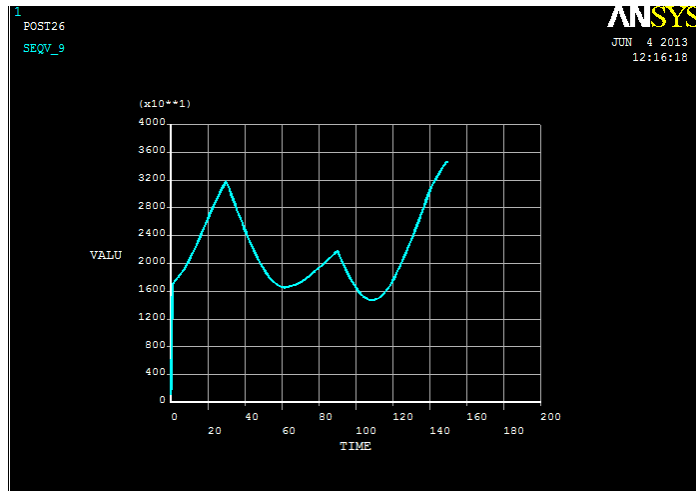


Figure 4.34 3rd Principal Stress plot for Case II

4.15 VALIDATION OF MODEL

The micro-models were validated next by a comparison with experimental results obtained from UPC (2009). Usually, experiments on load bearing walls have been adopted by the masonry community as the most common axial load test and the tensile capacity of masonry has been neglected. As a result, the clear understanding of the buckling characteristics of masonry load bearing walls under concentric and eccentric vertical load was absent.

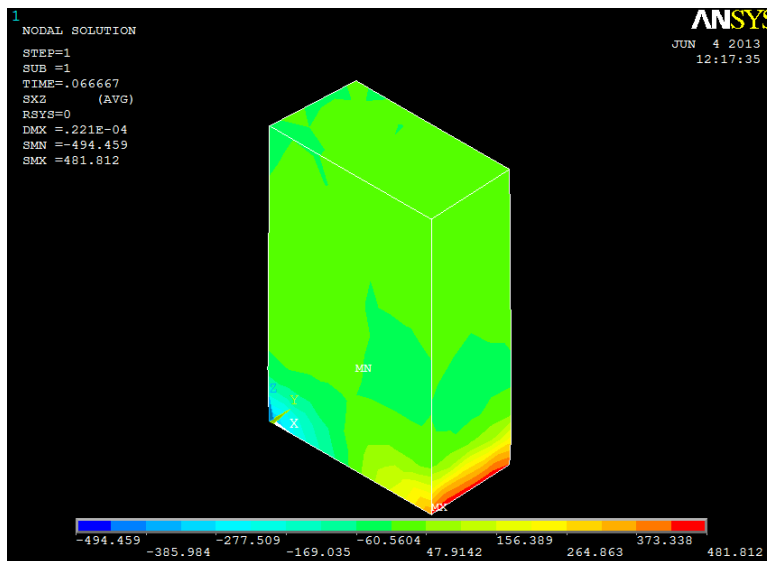


Figure 4.35 Z Shear Stress plot for Case II

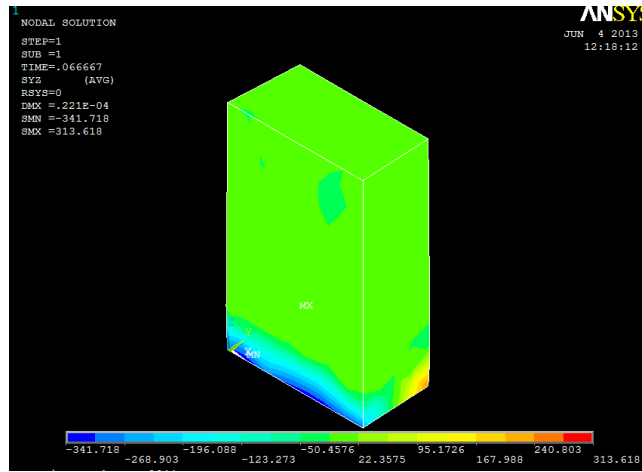


Figure 4.36 XY Shear plot for Case II

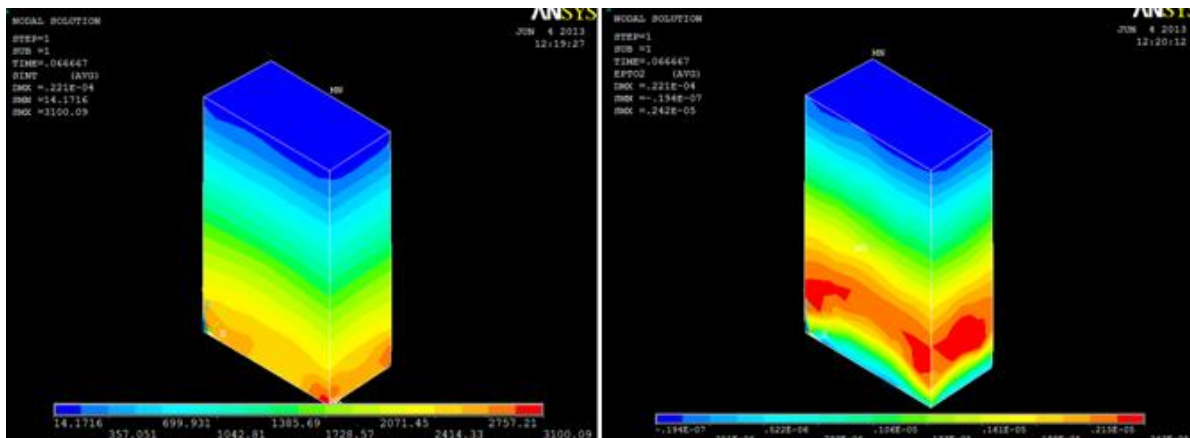


Figure 4.37 Stress intensity for (a) 2nd cycle of loading (b) 3rd cycle of loading



Figure 4.38 Cracking pattern under 2nd cycle of loading

It can be observed that simulation results of Case II are more closer to the actual model as compared to those of Case I. this can be attributed to the greater value of cohesion for the Drucker-Prager model. Also the flow angle has been reduced in Case II

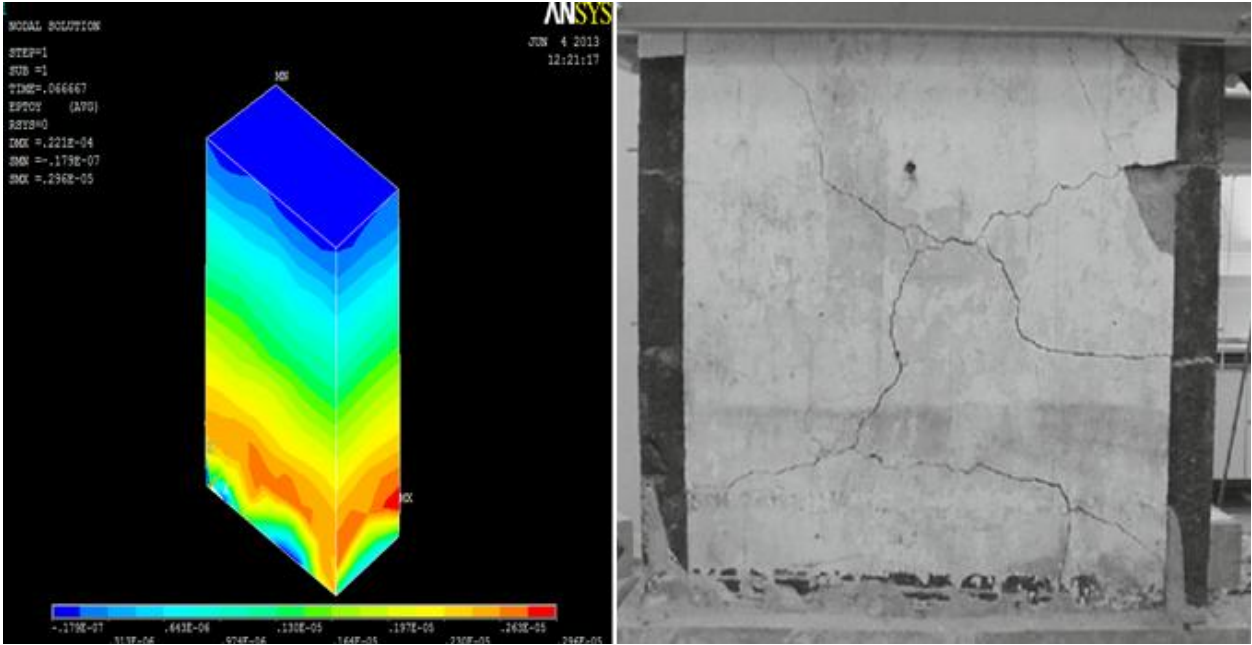


Figure 4.39 Comparison of Stress Concentration and Cracking pattern

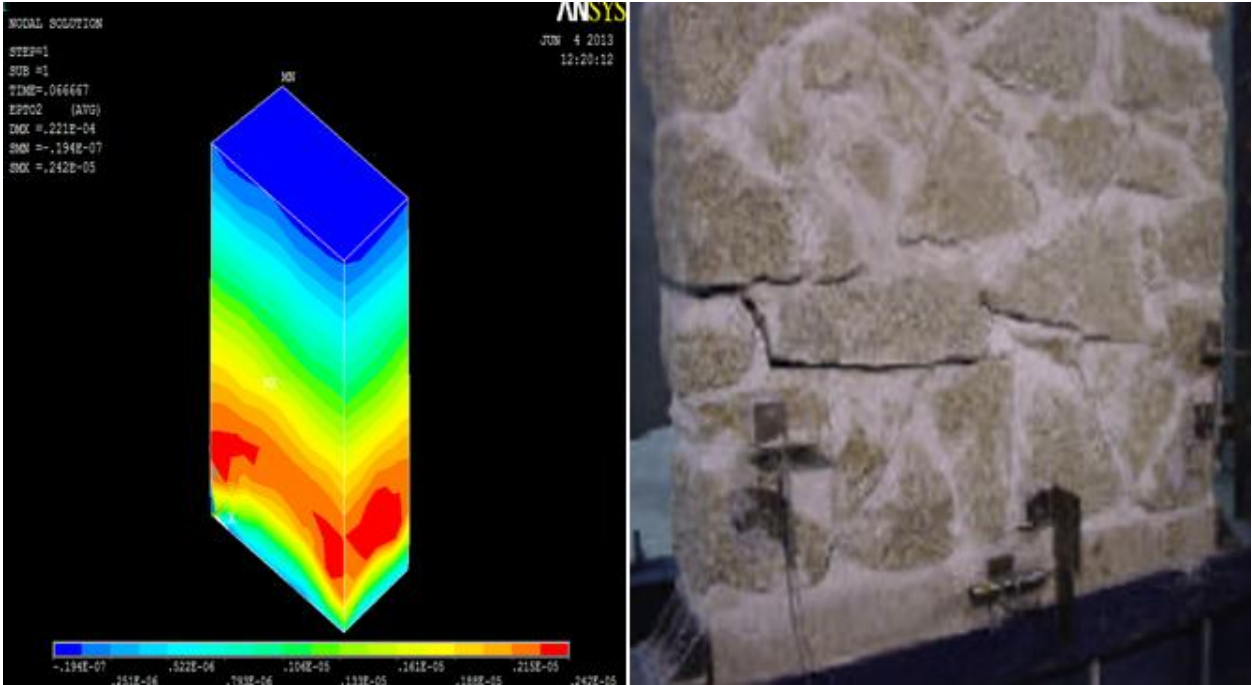
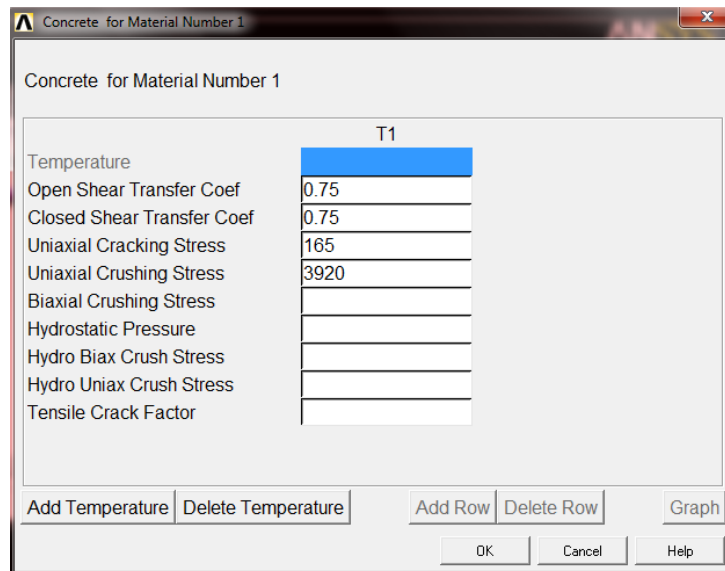
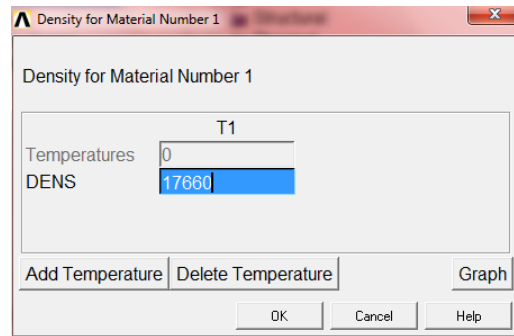
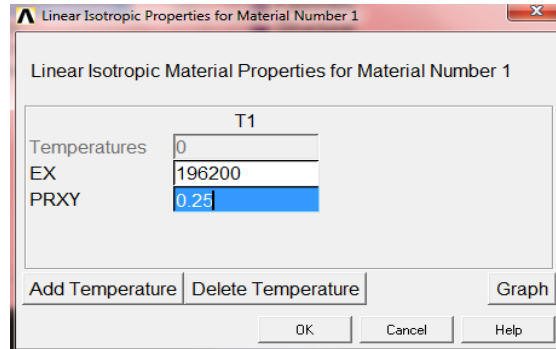


Figure 4.40 Comparison of Stress Concentration and Cracking patterns at higher loads

CASE III

- Elastic Modulus = 1.96 E+08 Pa
- Poisson's Ratio (XY) = 0.125
- Density = 17,660 N/m³

In Case III instead of simple Drucker Prager, WW (modified Tresca) model, was used.



In the above two cases, Drucker Prager model has been used for failure criteria under seismic loads. Although not included in this thesis document, many other tries were conducted for different values of cohesion, friction angle and flow angle in order to refine the results and make them more closer to the actual model. It was observed that beyond a certain degree of accuracy, the results could not be refined much despite changing the parameter values drastically.

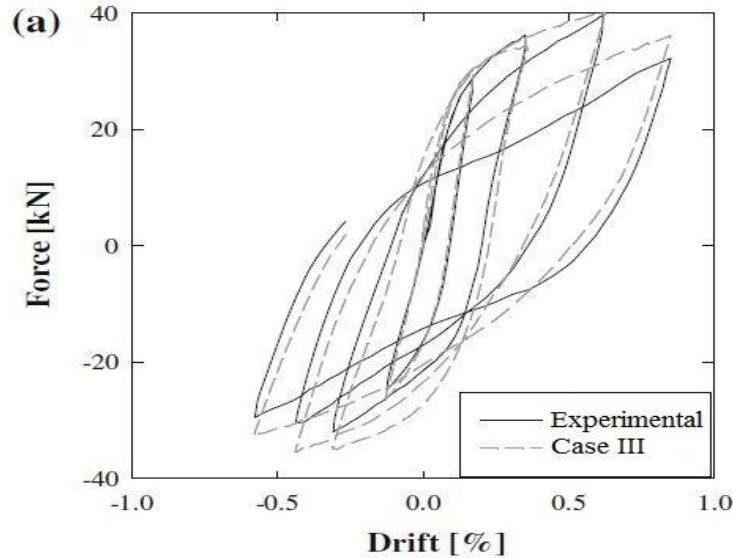


Figure 4.41 Storey Drift vs Force diagram for Case III

1
POST26
82_2

ANSYS
JUN 12 2013
10:39:03

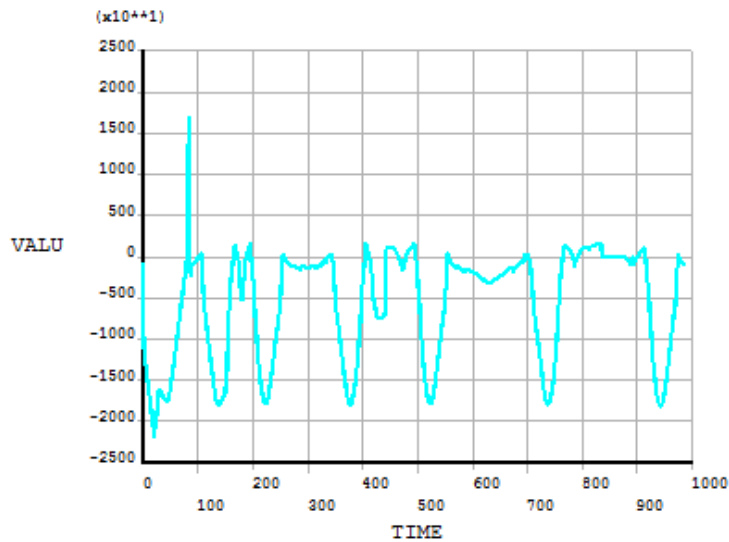


Figure 4.42 Time history of 2nd principle stress for Case III

For this reason another failure criterion, the WW failure criterion was incorporated into ANSYS through the following inputs:

Material Properties

E_m (modulus of elasticity): 0.1962 MPa

ν (poisson coefficient): 0.25

γ_m (masonry specific weight): 17.66 kN/m³

WW Failure Criterion

F_c (uniaxial compressive strength): 3.92 MPa

F_t (uniaxial tensile strength): 0.165 MPa

β_c (shear transfer coefficient for close cracks): 0.75

β_t (shear transfer coefficient for open cracks): 0.75

The following snap-shots illustrate different ANSYS windows for input of the afore mentioned values of different parameters.

1
POST26
33_3

ANSYS
JUN 12 2013
10:40:47

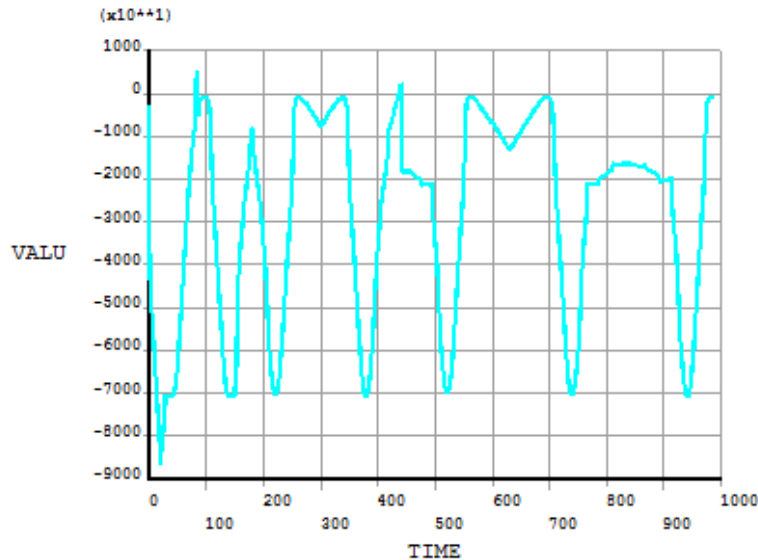


Figure 4.43 Time history of 3rd principle stress for Case III

1
POST26
SXY_4

ANSYS
JUN 12 2013
10:42:22

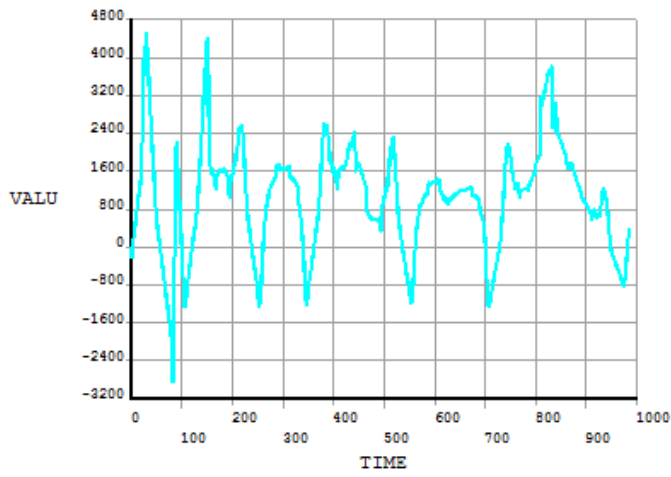


Figure 4.44 Time history of XY shear stress for Case III

1
POST26
EPELXY_7

ANSYS
JUN 12 2013
10:45:00

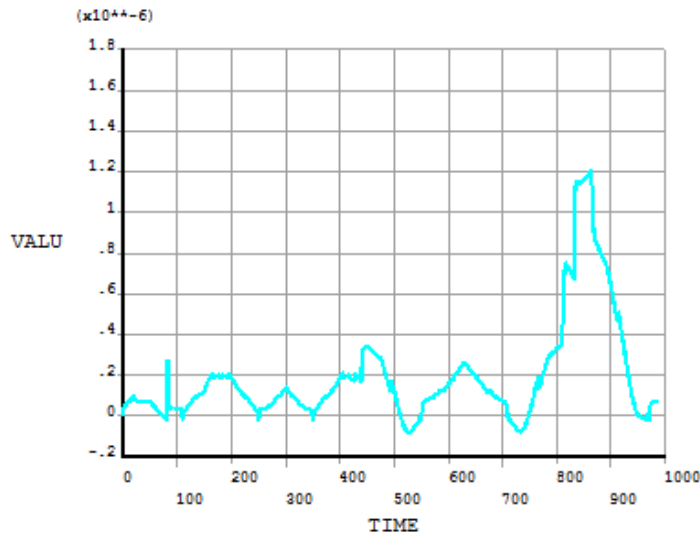


Figure 4.45 Time history of XY shear elastic stain for Case III

1
POST26
FY_11

ANSYS
JUN 12 2013
10:48:38

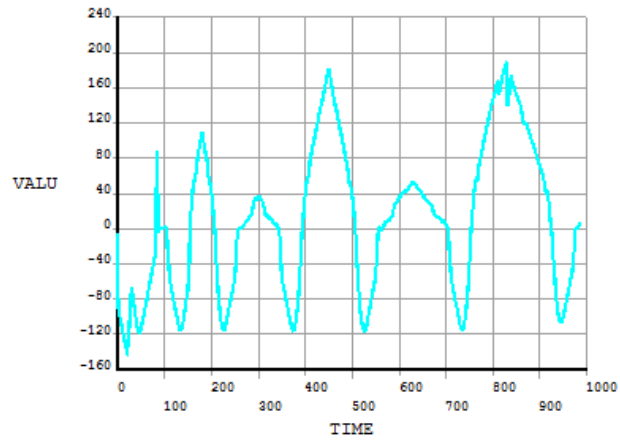


Figure 4.46 Time history of Y component of force for Case III

Case III results were plotted in similar comparisons but the elemental solution results were different from that of the Case I and Case II.

1
POST26
FOCV_13

ANSYS
JUN 12 2013
10:50:28

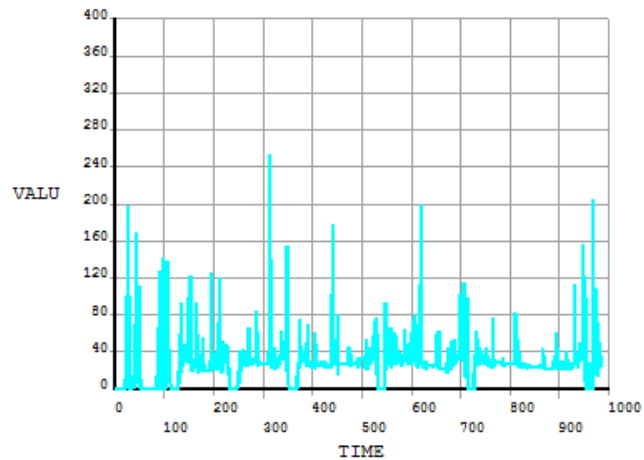


Figure 4.47 Convergence values for Force for Case III

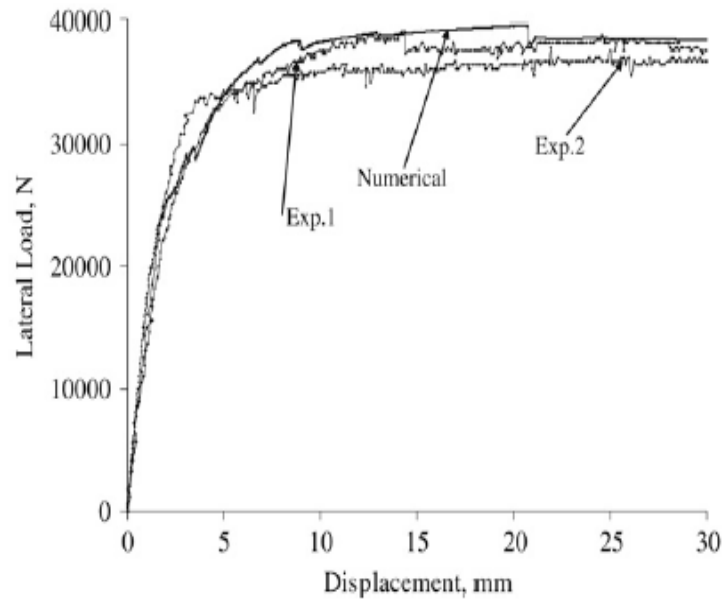


Figure 4.48 Comparison of numerical and experimental results for Case III

1
POST26
DICV_23

ANSYS
JUN 12 2013
10:53:51

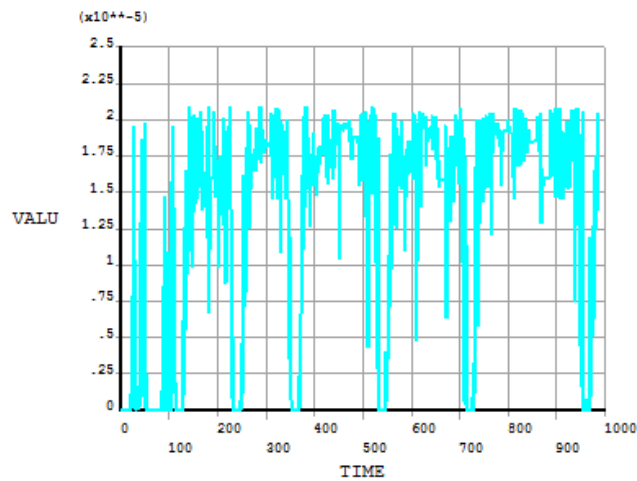


Figure 4.49 Convergence values for Displacement for Case III

Following comparisons show the cracking patterns in the real specimen and the concentration of cracking stresses in the FE model.

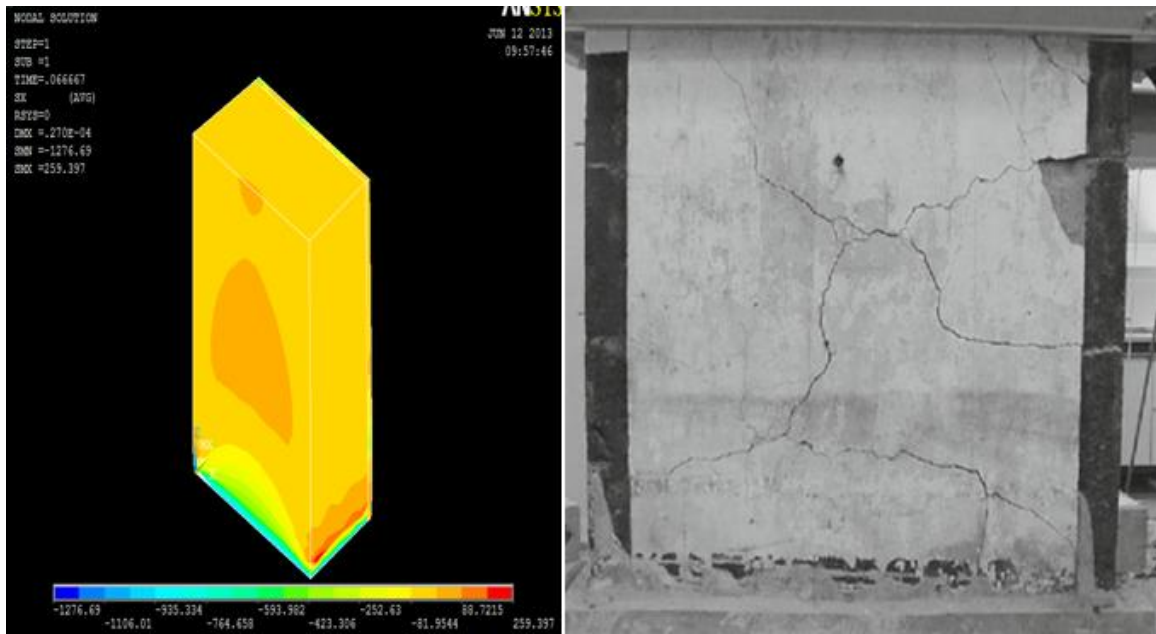


Figure 4.50 Principle Stresses build up at center and cracks in center of actual specimen

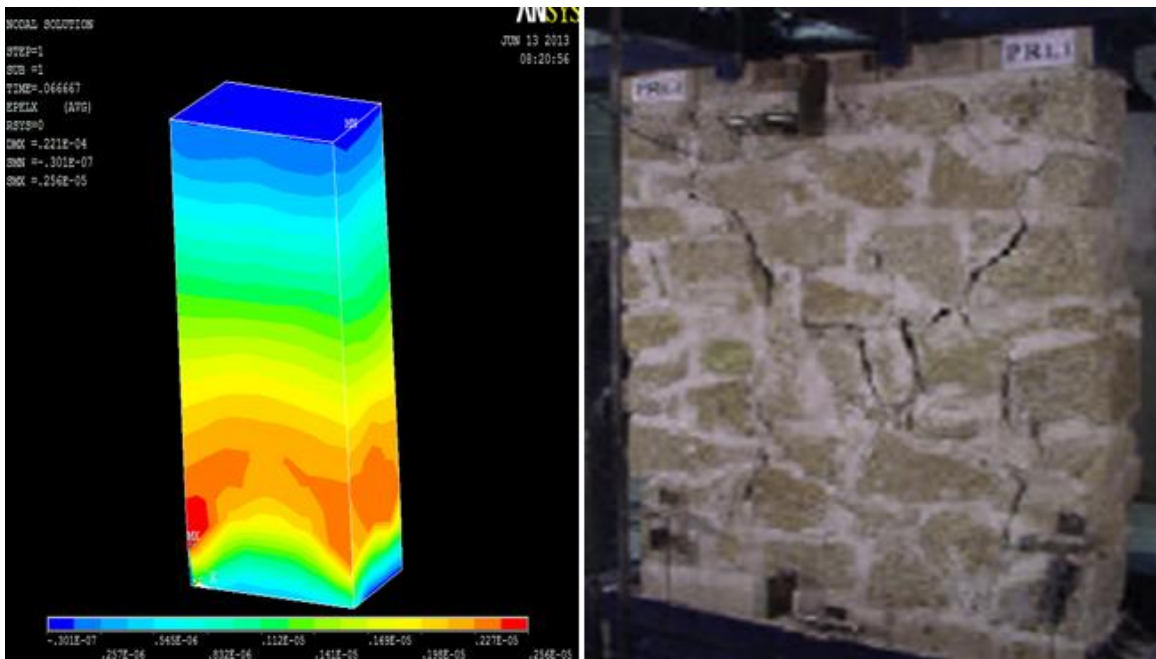


Figure 4.51 Comparison of cracks propagation at toe in model and actual specimen

CHAPTER 5

DISCUSSION ON RESULTS, CONCLUSIONS AND RECOMMENDATIONS

5.1 GENERAL

The effects of boundary condition and tensile strength on the failure load and buckling characteristics of masonry load bearing walls have been investigated by numerical parametric simulation. In the case of fixed support, the load capacity increased 2 to 6 times higher than hinge support depending on slenderness ratio and eccentricity. The capacity of wall for hinge-fixed support lies between the both end hinge and both end fixed support.

In the case of hinge-hinge support with high eccentricity, the influence of tensile strength is higher than the other support conditions. Most of the cases, negligible effect was found for null eccentricity. The influence of tensile strength follow a common tendency from higher to lower values when the support condition and load eccentricity moves from hinge to fixed and higher to lower eccentricity respectively.

These results make sense, however, further experimental tests and detail numerical simulation, to characterize the effect of end support conditions and tensile strength on buckling failure together with different slenderness ratio and load eccentricity, is recommended by the author.

Masonry is a material which exhibits distinct directional properties due to the mortar joints which act as planes of weakness. Large number of influence factors, such as anisotropy of units, dimension of units, joint width, material properties of the units and mortar, arrangement of bed as well as head joints and quality of workmanship, make the simulation of masonry difficult. The main objective of the present finite element modeling work was to evaluate analytically the in-plane seismic performance of three different types of stone masonry shear walls.

A plasticity theory based micro modeling techniques has been employed to carry out the analysis.

5.2 CONCLUSIONS

- Modified Drucker Prager model produces results for seismic response with precision of 8% more than that of simple Drucker Prager Model and WW model (modified Tresca Model)
- A nonlinear finite element method with 8-noded iso-parametric elements for combined masonry blocks and mortar joints gives 17% more accurate results when compared with that of an orthotropic element.
- Combined earthquake and low axial pre-compression loads caused flexural failures while higher pre-compression loads caused toe crushing and diagonal shear failures.

5.3 DISCUSSION ON CONCLUSIONS

- The analysis results showed that the failure patterns and load-deformation response of the shear walls are highly influenced by the by axial pre-compression and material properties. The strength of masonry is different for Case I, II and III but the behavior remain almost same particularly under higher axial pre-compression (175 kN and 250 kN). A nonlinear finite element method with 8-node iso-parametric quadrilateral elements for combined masonry blocks and mortar joints was used to predict the behavior of unreinforced masonry structures. The disturbed state concept of plasticity model with associated flow rules were used to characterize the compressive and tensile yields of the masonry structures. This paper presents the use of a model that allows for both compressive and tensile yields to analyze masonry structures. The model can account for micro-cracking in the masonry, which leads to softening and fracture.
- Lower axial pre-compression load caused flexural or rocking failures and higher pre-compression load caused rocking, toe crushing and diagonal shear failures along the diagonal direction. The predicted numerical failure modes are in good correspondence with the experimental failure modes. The numerical and experimental load-displacement diagrams are compared and presented.
- It has been observed that the WW model gives better results for stone masonry structures when analyzed with FE models. The numerically simulated cracking pattern for WW model is more close to that of the actual model as seen from the literature above.
- Multi-linear elastic material can also be used for modeling masonry but it would require exact calculation of failure stress and strain values to be incorporated into the software.

5.4 RECOMMENDATIONS

- The plasticity model involves two separate yield surfaces for compressive and tensile yield; the continuous nature of the proposed yield surface avoids computational difficulties in currently available discontinuous or multiple surfaces models, such as critical state and cap models. The model allows for the generation of discontinuities in the material microstructure during loading (unloading), and it does not require external enrichments to allow coupling between continuous and discontinuous parts within the deforming material.
- Moreover, the same framework can be used to model the behavior of interfaces and joint. The model for masonry was validated at the specimen level. It was also applied successfully for a number of unreinforced masonry prism specimens. The model can predict the hardening and softening behavior of materials. In addition, a closed form solution was proposed based on the calibrated parameters of the model. The closed form solution predicts the ultimate lateral load of an unreinforced masonry wall relatively well. Therefore, the model can be used satisfactorily to analyze masonry structures similar to those considered herein.
- Drucker Prager and WW models when applied to continuous surface avoids computational difficulties in currently available discontinuous or multiple surfaces models, such as masonry models. Hence, it should be preferred for time-efficient FE analysis of masonry structure.
- With little modifications, the input parameters of this model can be used satisfactorily to analyze masonry structures similar to those considered herein such as brick masonry and block masonry structures.

REFERENCES

- Abrams, D.P., and Shah, N. 1992. Cyclic Load Testing of Unreinforced Masonry Walls, Advanced Construction Technology Center Rep.No.92-26-10, College of Engineering, Univ. of Illinois at Urbana-Champaign, Advanced Construction Technology Center, Urbana,
- Ahmad Hussain 2006, "A Segment of Main Boundary Thrust Triggered October 08, 2005 earthquake, Pakistan" Workshop on earthquake vulnerability and multi hazard risk assessment held at NCEG Peshawar, November 2006.
- Alcocer, S.M., and Klingner, R.E., "Masonry Research in the America", Masonry Research in Americas, ACI(SP-147), pp, 239-262.
- Alcocer, S.M., Arias, J.G., Vazquez, A., "Response Assessment of Mexican Confined Masonry Structures Through Shaking Table Tests", proc. 13th World Conference on Earthquake Engineering, Vancouver, B.C., Canada, paper No. 2130.
- Ali, Qaisar. 2004. Seismic Performance Study of Brick Masonry Building Systems in Peshawar Region, PhD Thesis, Department of Civil Engineering, UET, Peshawar.
- Ambraseys, N.N.J. Dougals, S.K. Sarma, and P.M. Smit 2005 "Equations for the Estimation of Strong Ground Motions from Shallow Crustal Earthquakes Using Data from Europe and the Middle East: Vertical Peak Ground Acceleration and Spectral Acceleration" Bulletin of Earthquake Engineering 3:55-73.
- Amr S. Elnashai and Luigi DiSarno. "Fundamentals of Earthquake Engineering" 2008 John Wiley & Sons, Ltd.
- Anthoine, A., Magonette, G., and Magenes, G. 1995. Shear Compression Testing and Analysis of Brick Masonry Walls, Proc., 10th European Conf. on Earthquake Engineering, Taylor and Francis, Rotterdam, The Netherlands, 1657-1662. Application to shear walls. Proceedings of British ceramic society, Vol.30, pp.223-235, 1982.
- Chopra, A. K. (2000). Dynamics of Structures: Theory and Applications to Earthquake Engineering. Prentice Hall, New Jersey.
- Cleveland, L. (2006). Seismic Loss Assessment for the New Madrid Seismic Zone, Department of Civil and Environmental Engineering. Urbana, IL, University of Illinois at Urbana-Champaign.

Coburn A. and Spence R.: "Earthquake Protection". John Wiley & Sons, Chichester, 1992.

Costley, A. C., and Abrams, D. P. 1996. Dynamic Response of Unreinforced Masonry Buildings with Flexible Diaphragms, NCEER-96-0001, Univ. of Buffalo, Buffalo, USA

Craig, J., Goodno, B., Towashiraporn, P., and Park, J. 2002. Fragility Reduction Estimations for URM Buildings Using Response Modification, Proc., 12th European Conf. on Earthquake Engineering Research, London, Paper No. 805.

Eurocode 6: Design of masonry structures, Part 1-1: Common rules for reinforced and unreinforced masonry structures. ENV1996-1-1:2004:E (CEN, Brussels)

European Macroseismic Scale 1998, Centre Européen de Géodynamique et de Séismologie, Luxembourg, 1998.

Faccioli E., Pessina V., Calvi G.M. and Borzi B.: "A study on damage scenarios for residential buildings in Catania city". Journal of Seismology, Vol. 3, No. 3, 1999.

Fah, D., F. Kind, et al. (2001). Earthquake Scenarios for the City of Basel, Soil Dynamics and Earthquake Engineering, 21(5), 405-413.

Fajfar, P. 2000. "A Nonlinear Analysis Method for Performance-Based Seismic Design" Earthquake Spectra 16(3), 573-592.

Magenes, G., and Calvi G.M. 1997. In-Plane Seismic Response of Brick Masonry Walls, Earthquake Engineering and Structural Dynamics, Vol. 26, 1091-1112

Magenes, G., Kingsley G.R. and Calvi G.M. 1995. Seismic Testing of a Full-scale, Two-storey Masonry Building: Test Procedure and Measured Experimental Response, Università degli Studi di Pavia.

Manzouri, T., Shing, P.B., Amadei, B., Schuller, M., and Atkinson, R. 1995. Repair and Retrofit of Unreinforced Masonry Walls: Experimental Evaluation and Finite Element Analysis. Rep. No. CU/SR-95/2. Department of Civil, Environmental and Architectural Engineering, University of Colorado, Boulder, Colorado

Mid-America Earthquake Center (MAE Center), 2007. Mid-America Earthquake Center Seismic Loss Assessment System, MA Eviz v3.1.1, University of Illinois at Urbana-Champaign, Urbana, IL

Porro B. and Schraft A.: "Investigation of insured earthquake damage". *Natural Hazard*, Vol2, pp.173-184, 1989.

Ramos, L.F. and P.B. Lourenco (2004). *Modeling and Vulnerability of Historical City Centers in Seismic Areas: A Case Study in Lisbon*. *Engineering Structures* 26(9), 1295-1310.

Rashid Ullah "Seismic Hazard Analysis (SHA) For Design of Structures in Islamabad" M.Sc. Thesis, University of Engineering and Technology, Peshawar, Pakistan, 2010.

Reiter, L. [1990], "Earthquake hazard analysis-issues and insights", Columbia University Press, New York, 254pp.

Shibata T 1970 Analysis of liquefaction of saturated and during cyclic loading *Disaster Prevention Res.Inst. Bull.* 13 563-70

Tantala, M.G. Nordenson, et al. (1999-2003). *Earthquake Risks and Mitigation in the New York, New Jersey and Connecticut Region*, The New York City Area Consortium for Earthquake Engineering

Tianyi, Yi. 2004. *Large-scale Testing of a Two Storey URM Structure*. PhD Dissertation, Atlanta: Georgia Institute of Technology.

Turnšek V. and Sheppard P.: "The shear and flexural resistance of masonry walls". *Proceedings of International Research Conference on Earthquake Engineering*, Skopje, 1980. W.F. Chin & Charles Scawthorn, 2003. *Earthquake Engineering Hand Book*, CRC 2003, pp 2-5.

Wen, Y. K., B. R. Ellingwood, et al. (2004a). *Vulnerability Function Framework for Consequence-Based Engineering*. Urbana, IL, Mid-America Earthquake (MAE) Center.

Wen, Y. K., B. R. Ellingwood, et al. (2004b). *Vulnerability Functions*. Urbana, IL, Mid-America Earthquake (MAE) Center.

Whitman R.V., Reed J.W. and Hong S.T.: "Earthquake damage probability matrices". *Proceedings of the fifth World Conference on Earthquake Engineering*, pp.2531, Rome, 1974.